Body Weight Support

Influence on lateral balance

Nathan Fopma

Technische Universiteit Delft

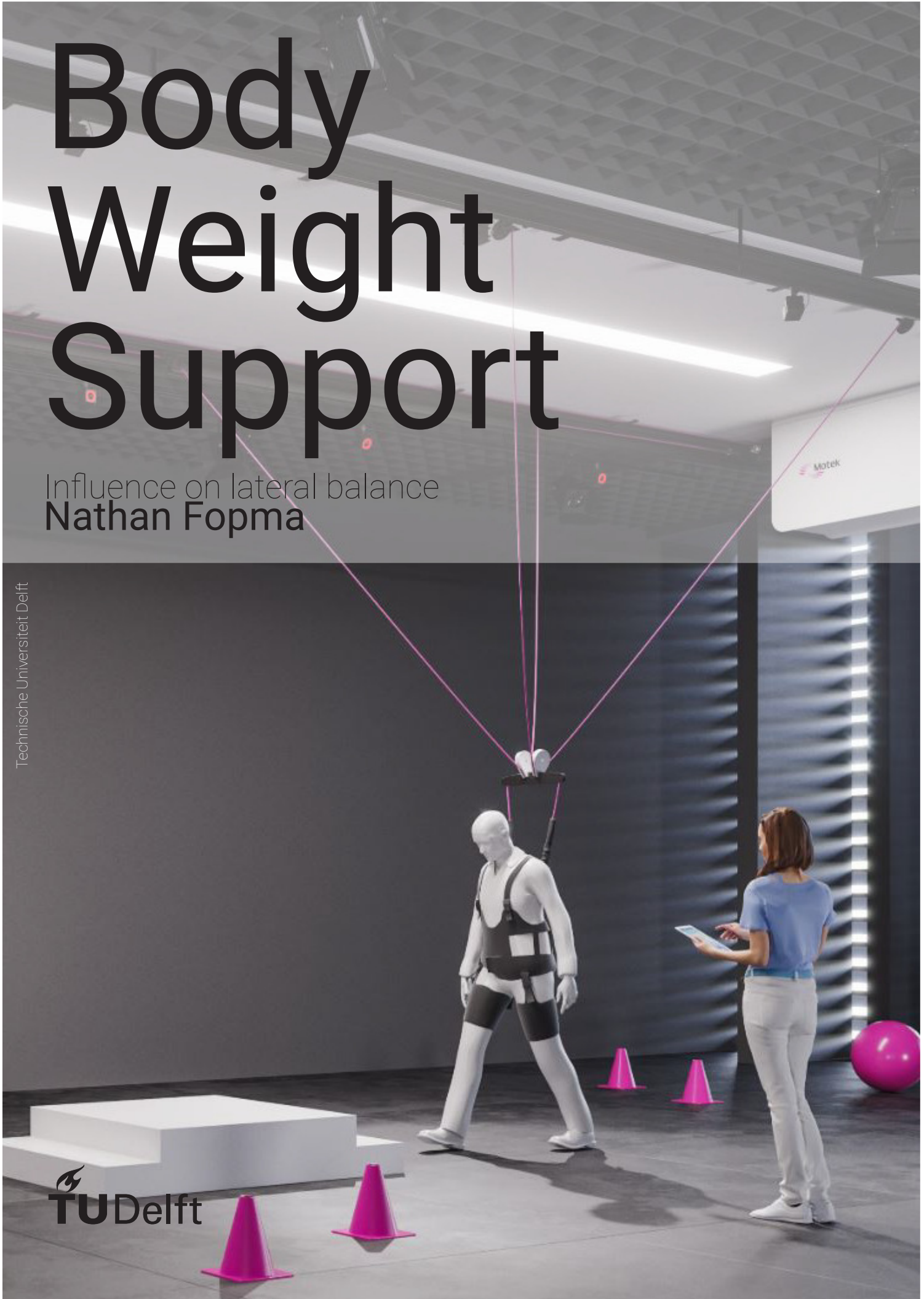

TU Delft

Body Weight Support

Influence on lateral balance

by

Nathan Fopma

to obtain the degree of Master of Science
at the Delft University of Technology,
to be defended publicly on Thursday April 9, 2020 at 14:00.

Student number:	4163664		
Project duration:	October 1, 2018 – April 9, 2020		
Thesis committee:	Prof. dr. ing. H. Vallery,	TU Delft	Supervisor
	Ir. A. Barry,	TU Delft	Daily supervisor
	Prof dr. ir. D. A. Abbink,	TU Delft	External committee member

An electronic version of this thesis is available at `http://repository.tudelft.nl/`.

TU Delft

Preface

I am glad that I can finally present to you the final work of my master's Biomechanical Design. After working in a student team on the development of an exoskeleton after my bachelor's, I was motivated to develop further my understanding of the interaction between humans and assistive technology. I am glad that I chose this path and could not have thought of a better way to conclude my time in Delft.

Especially, I want to thank my daily supervisors throughout the final graduation year. Starting in October 2018, Patricia was my first supervisor. She helped me with starting up this year of research, define the scope of the project, and gave me valuable – technical and mental – support during my literature review. From February 2019 onwards, Andy took over this role until my graduation now. Andy, your supervision has helped me tremendously in the past year. You were always open for a discussion, took a lot of time to help me clear-up my ideas, and guided me into learning the skill of scientific storytelling. With your guidance and extensive comments, my thesis and literature review turned into works that I can be proud of. It was a real pleasure working with you.

Heike, the weekly meetings that we had were immensely helpful. I am glad that I could often walk by your office and quickly have your feedback or thoughts about a problem on my mind. Your critical attitude motivated me to do my utter best. Your enthusiasm and curiosity towards research made my time working on the thesis delightful. I will always remember your inspiring vision about assistive technology. We should strive to create devices that are within reach of the people we ought to help. Also, thank you for trusting me in the role of lab manager.

David, thanks for being a part of my graduation committee. From all of my master's courses, I enjoyed yours most – your dedication and style of education were stimulating. Thanks for your referral to the Delft Biorobotics Lab for my internship. Without that, I would not have landed on this graduation topic.

The atmosphere in the Biorobotics Laboratory is one that completely exceeded my expectations. I have heard of no other students who had such a bright social experience during their master graduation project. I want to thank my fellow MSc students (Christine, Aneesh, Joris, Roemer, Ashwin), visiting researchers (Romain, Charlotte, Lucy, Christian, Krittika, Carlos), and resident PhD students and post-docs (Andy, Daniel, Patricia, Saher, Bram) for their contribution to the open atmosphere in the lab. I greatly enjoyed all the lunches, coffee breaks, Feuerzangebowlen, and VrijMiBos we had together.

I am thanksful for my family and friends being by my side through the ups and downs of my bachelor's, master's, and other projects. Especially, I want to thank my girlfriend Michelle, and my housemate Gijs. Thank you for all the kitchen table and late-night conversations that helped me through several rough patches. I am grateful for the support of my mother, father, stepfather, and sister throughout my studies. I am happy that you allowed me to freely follow my curiosity. This freedom allowed me to get a firm grasp on what motivates me, and what I think is important in life. With all this new knowledge, I am excited to see what the rest of my life will bring.

Nathan Fopma
Delft, March 2020

Contents

Table 1. Nomenclature

Abbreviation	Definition
BW	Bodyweight
BWS	Bodyweight Support
ML	Mediolateral
CoM	Center of Mass
CoM'	Projection of CoM on the ground
XCoM	Extrapolated Center of Mass
CoP	Center of Pressure
LF	Laterally Fixed
LG	Laterally Guided
$\boldsymbol{F}_{\text{BWS}}$	BWS Force vector
$F_{\text{BWS}x}$	ML component of the $\boldsymbol{F}_{\text{BWS}}$
$F_{\text{BWS}y}$	Vertical component of the $\boldsymbol{F}_{\text{BWS}}$
$\boldsymbol{F}_{\text{GRF}}$	Ground Reaction Force vector
$F_{\text{GRF}x}$	ML component the $\boldsymbol{F}_{\text{GRF}}$
$F_{\text{GRF}y}$	Vertical component the $\boldsymbol{F}_{\text{GRF}}$
m	Mass of the whole body
g	Gravitational Constant
x_{CoM}, $\ddot{x}_{\text{CoM}}$	ML position/acceleration of the CoM
y_{CoM}, $\ddot{y}_{\text{CoM}}$	Vertical position/acceleration of the CoM
$\theta, \ddot{\theta}$	Rotation and angular acceleration of the whole body around the CoM
x_{CoP}	ML position CoP
x_{BWS}	ML position of point of application the $\boldsymbol{F}_{\text{BWS}}$
y_{BWS}	Vertical position of point of application the $\boldsymbol{F}_{\text{BWS}}$
x_{SP}	ML position of the suspension point of the BWS system
y_{SP}	Vertical position of the suspension point of the BWS system
T_{i}	Torque around CoM created by counter-rotation strategy
I_{CoM}	Rotational inertia of the whole body around the CoM
l_{eq}	Equivalent pendulum length

Influence of Vertical and Lateral Bodyweight-Support Forces on Lateral Balance

Nathan Fopma
Supervised by: Andrew Berry, Heike Vallery[1] ✉

[1]Faculty of Mechanical, Maritime, and Materials Engineering - Biomechanical Engineering. TU Delft, 2628 CD Delft, The Netherlands

Bodyweight-supported gait training enables functional and task-specific training of walking shortly after a neurological injury. After a neurological injury, individuals have to relearn their active control of lateral balance to avoid falling. However, bodyweight-support forces seem to influence the dynamics of lateral balance. Existing literature does not sufficiently explain the interplay between bodyweight support and lateral balance, and conflicting results have been reported. One possible explanation of the inconsistent results is the concurrent application of vertical unloading and lateral support forces. This manner of force application is inherent to the mechanics of most bodyweight-support systems. This experiment aims to study the independent effect of vertical and lateral bodyweight-support forces on lateral balance.

A RYSEN (Motek Medical B.V., Amsterdam, The Netherlands) bodyweight-support system was used, which allows the independent control of vertical unloading and lateral support forces. Fifteen participants walked overground in six different unloading conditions of the RYSEN. In the first part of the experiment, the vertical unloading force was increased, while no active lateral support forces were applied. In the second part of the experiment, the vertical unloading force was kept at a constant value, while the lateral support forces were changed. Gait characteristics related to lateral balance were extracted from motion capture and force plate data.

Increasing the vertical unloading had a significant effect on the step width, center of mass displacement and velocity, margin of stability, foot progression angle, and the relative time spent in the double support phase. An analysis that used the equations of motion for human walking revealed that the contribution of the foot-placement and ankle strategy to the mediolateral ground reaction force decreased due to unloading. This decrease may have been caused by an increased use of the counter-rotation strategy to control lateral balance. However, further analysis showed how the lateral alignment of the body weight support force with the center of mass biased this analysis. Lateral support showed much less effects than expected from literature. This seemed to be caused by the lateral support conditions producing too similar support forces.

Bodyweight Support | Bodyweight Unloading | Lateral Balance | Frontal Plane Balance | Balance Strategies
Correspondence: ***n.c.fopma@student.tudelft.nl***

1: Introduction

A. Bodyweight Support and Lateral Balance. After a neurological injury, such as stroke or an impartial spinal cord injury, the ability to independently stand up, walk, and remain balanced, can be severely impaired (Langhorne et al. (2009)). This impairment drastically reduces mobility and creates a reliance on disability aids, medical professionals, friends, and relatives. Walking is a complex neural control mechanism that is difficult to restore after neurological trauma (Barbeau and Fung (2001)). In many cases, patients must regain their strength to withstand gravity and their ability to remain balanced (Tyson et al. (2006)).

Effective bipedal locomotion requires balance. Balance during walking is defined as remaining upright and avoid falling (Bruijn et al. (2013)). The analysis of passive-dynamic walkers by MacGeer (1990) suggests that balance in the sagittal plane is passively stable. A small perturbation to a passive 2D walker on an incline slope is dissipated in subsequent steps, without the need for active control. Kuo (1999) found that this passive stability does not extend to the frontal plane, which means that humans have to actively control their motion in the mediolateral (ML) direction to remain balanced. Poor ML balance is a predictor of future falls in olders adults (Hilliard et al. (2008)). For the elderly, a fall in the ML direction carries a high risk of hip fracture, which can lead to long-term immobilization (Nankaku et al. (2005)).

Bodyweight Support (BWS) is a valuable tool for rehabilitation. BWS systems reduce the load on the legs by providing a vertical support force acting against gravity. In most of these systems, users wear a harness that is suspended by a cable system. A support force is generated by tensioning the cable. The amount of unloading during BWS training is commonly expressed as a percentage of the bodyweight (BW). Most commercial systems provide unloading forces in the range between 5% and 70% of the BW. By unloading part of the BW, BWS devices reduce the required muscle forces to stand and walk. This unloading enables functional and task-specific training of locomotion at an early stage of the rehabilitation process (Hesse (2008)). Moreover, the systems create a feeling of safety for the patients, enabling them to explore the walking motion without the fear of falling (Miller et al. (2012)).

Bodyweight-supported training of walking can be achieved by either suspending the user from a fixed point above a treadmill or by allowing the suspension point to translate along a rail to enable overground walking. These overground systems, however, constrain the movement of the user to walking along the path of the guiding rail. More advanced BWS systems have been developed that guide the suspension point both in the anterior-posterior and ML direction, such as the FLOAT (Reha-Stim Medtec AG,

Schlieren, Switzerland, Vallery et al. (2013)) and the RYSEN (Motek Medical B.V., Amsterdam, The Netherlands, Plooij et al. (2018)).

Humans walk energetically efficient when they walk with a step width, because this avoids that the swing leg has to actively circumduct the support leg during walking (Donelan et al. (2001)). Walking with a step width causes the Center of Mass (CoM) to oscillate from left to right. When the amplitude of this oscillation exceeds the lateral border of the support foot, humans must react by making a cross-step, which can lead to a fall by tripping. To remain balanced, a human has to contain the ML CoM oscillation inside the lateral edge of the base of support, which is formed as the convex hull of the foot area in contact with the ground.

Mackinnon and Winter (1993) described three strategies to control the CoM in the frontal plane during walking. They based their analysis on an inverted pendulum model where the ankle joint is the base of the pendulum. Mainly, the 'foot-placement strategy' is employed: lateral placement of the supporting limb creates a lever arm between the center of mass and the supporting ankle; the force of gravity hence produces angular acceleration of the body around the ankle joint. After foot placement, a human can fine-tune their CoM control by creating an extra inversion/eversion moment around the ankle joint ('ankle strategy') or by rotating body segments about the CoM and exerting horizontal ground reaction forces ('counter-rotation strategy', Hof (2007)). Examples of the latter strategy include rotation of the upper body about the hip joint (Horak and Nashner (1986)) or swinging of the arms (Pijnappels et al. (2010)).

Mackinnon and Winter (1993) showed that the foot-placement strategy contributes the most to ML CoM motion during regular steady-state gait. Kuo (1999) calculated that the foot-placement strategy requires the least amount of energy to dissipate possible perturbations. Hof et al. (2005) modeled how humans use their foot placement to maintain lateral balance. They model the frontal plane stance phase of human walking as a linearized inverted pendulum. With each step, there exists precisely one position to place the foot that causes the body to come to rest at the upright pendulum position. This position is called the 'Extrapolated Center of Mass' (XCoM) and is computed from the CoM position and velocity. To keep lateral balance, a human must always step lateral to this XCoM. In subsequent experiments, Hof et al. (2010) studied the effect of ML perturbations to the pelvis during treadmill walking on the ankle and foot-placement strategies. They found that humans place their feet predictably at a certain distance to the XCoM. This distance is called the 'Margin of Stability'. Secondly, they conclude that even though the ankle strategy is able to react to perturbations faster than foot placement, the foot-placement strategy is more effective because it can create much larger restoring forces than the ankle strategy.

Although intended to only provide vertical support, most BWS systems seem to provide lateral support forces. Pennycott et al. (2011) noted that BWS systems with a Laterally Fixed (LF) suspension point provide a laterally stabilizing force during walking. Fig. 1a shows this lateral stabilization – when the harness moves laterally to the suspension point, the BWS force ($\boldsymbol{F}_{\mathrm{BWS}}$) is applied at an angle, which creates an ML component of the force ($F_{\mathrm{BWS}x}$). In this article, the x and y coordinates represent respectively the ML and vertical axes. Because the CoM oscillates from left to right during walking, this mechanism causes a spring-like lateral restoring force to be applied to the human. In contrast, Fig. 1b shows a system that has a Laterally Guided (LG) suspension point, such as the RYSEN or the FLOAT, which actively tracks the lateral position of the suspension point and therefore provides a more vertical unloading force. Donelan et al. (2004) state that lateral support during regular walking seems to decrease the requirements to actively control lateral balance. In their experiment, they applied a lateral stiffness to the pelvis of healthy participants and found a decrease in step width, step width variability, and lateral CoM displacement. The external stabilization also decreased the metabolic cost of walking. Several other experiments concluded similar results: step width and its variability decrease when a lateral stiffness is applied to the pelvis (Dean et al. (2007), IJmker et al. (2014), Matsubara et al. (2015)).

The vertical unloading force also seems to affect lateral balance. Dragunas and Gordon (2016) note that the foot-placement strategy depends on the force of gravity. The lateral foot placement creates a lever arm for the force of gravity, which accelerates the whole body around the ankle joint. Because the vertical unloading force opposes the force of gravity, this decreases the effectiveness of the normally dominant foot-placement strategy. This means that both the vertical unloading and lateral support during BWS training influence lateral balance, which could be unfavorable for relearning lateral balance during rehabilitation.

Interpreting the effect of BWS on lateral balance from previously published literature can be difficult. Most commonly, LF BWS systems are used, which provide both vertical unloading and lateral support at the same time. There seems to be agreement on the fact that the ML CoM motion is attenuated by BWS regardless of the lateral suspension type. However, contradicting results are reported for the effect of BWS on lateral foot placement. Aaslund and Moe-Nilssen (2008) showed that LF BWS decreases the ML acceleration of the CoM. Fischer and Wolf (2016) observed that the CoP moves more laterally during the single stance phase when LF unloading is provided, which suggests more use of the ankle strategy. Dragunas and Gordon (2016) found that LF BWS causes an increase of the step width and a decrease of step width variability. Van Thuc and Yamamoto (2017) detected a decreased step width and ML CoM displacement when both LF and LG unloading are provided. They observed a larger decrease of the ML CoM displacement when LF unloading is provided. Easthope et al. (2018) noticed that LG unloading caused a decrease in the CoM displacement for healthy humans and iSCI patients. They found a decrease in step width for healthy humans.

B. Research Goals. The interplay between BWS and lateral balance is not yet sufficiently understood. One possible explanation might be the common use of LF BWS devices, which provide both vertical unloading and lateral support concurrently. In this experiment, we aim to gain a deeper understanding on the independent effect of vertical and lateral BWS forces on lateral balance. The first part of the experiment will study the effect of increased vertical unloading while the lateral support forces are kept at a minimum. In the second part of the experiment, lateral support is provided through lateral stiffness and damping, while the vertical unloading stays constant.

We expect several effects of the vertical unloading force. Dragunas and Gordon (2016) noted that vertical BWS forces make it more difficult for humans to stabilize their CoM by using their foot-placement strategy. Therefore, assuming that the foot-placement strategy requires a similar restoring moment around the ankle joint, vertical unloading should increase the required step width. However, due to an increased energetic cost when walking with a wider step width (Donelan et al. (2002)), we hypothesize that alternative balancing strategies will partially compensate for this. Step width variability reflects the feedback control task of foot placement (Beauchet et al. (2009)). Higher demands for lateral stabilization by the foot-placement strategy would increase the control effort required for the foot placement task, which would reflect as a higher step width variability with increased vertical unloading.

Our expectations for the effect of lateral support during BWS aligns with the literature on lateral support during regular walking: they decrease the requirements to actively control lateral balance. This would show as a decreased step width, step width variability, and lateral CoM motion.

2: Methods

A. Modeled Influence of BWS on Lateral Balance. Hof (2007) derived the equations of motion for human postural balance. These equations of motion are used to understand the influence of BWS on lateral balance. Under the feet, a Ground Reaction Force ($\boldsymbol{F}_{\mathrm{GRF}}$) applies, whose point of application is the Center of Pressure (CoP). Fig. 2a shows the free-body diagram for regular human walking. From this diagram, the lateral and vertical force balances can be derived as

$$\sum F_x = m \cdot \ddot{x}_{\mathrm{CoM}} = F_{\mathrm{GRF}x} \tag{1}$$

$$\sum F_y = m \cdot \ddot{y}_{\mathrm{CoM}} = F_{\mathrm{GRF}y} - mg. \tag{2}$$

The frontal-plane moment balance around the CoM is

$$\begin{aligned}\sum M_{\mathrm{CoM}} &= I_{\mathrm{CoM}} \cdot \ddot{\theta} \\ &= y_{\mathrm{CoM}} \cdot F_{\mathrm{GRF}x} + (x_{\mathrm{CoP}} - x_{\mathrm{CoM}}) \cdot F_{\mathrm{GRF}y} + T_{\mathrm{i}},\end{aligned} \tag{3}$$

where T_{i} is an inertial torque around the CoM defined by Hof (2007), which is created by accelerating body segments with respect to the CoM through the counter-rotation strategy. Human walking in the frontal plane can be modelled as a linearized inverted pendulum with a length l, where $y_{\mathrm{CoM}} = \cos\theta l \approx l$. For this model, the angular and linear acceleration of the CoM are coupled as

$$\ddot{\theta} = -\frac{\ddot{x}_{\mathrm{CoM}}}{y_{\mathrm{CoM}}}. \tag{4}$$

If Eq. (4) and $F_{\mathrm{GRF}x} = m\ddot{x}_{\mathrm{CoM}}$ from Eq. (1) are substituted into Eq. (3), we get the following expression

$$-\left(\frac{I_{\mathrm{CoM}}}{m y_{\mathrm{CoM}}} + y_{\mathrm{CoM}}\right) \cdot m\ddot{x}_{\mathrm{CoM}} = (x_{\mathrm{CoP}} - x_{\mathrm{CoM}}) \cdot F_{\mathrm{GRF}y} + T_{\mathrm{i}}. \tag{5}$$

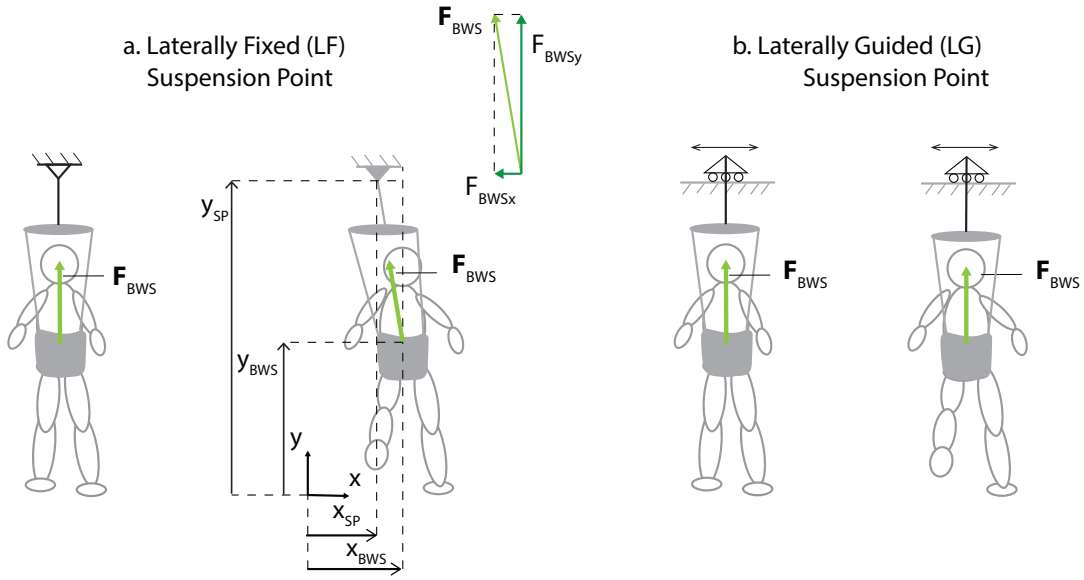

Fig. 1. The BWS force has a different direction in a laterally fixed suspension point system than in a laterally guided suspension point system. The location of the suspension point is represented by x_{SP} and y_{SP}.

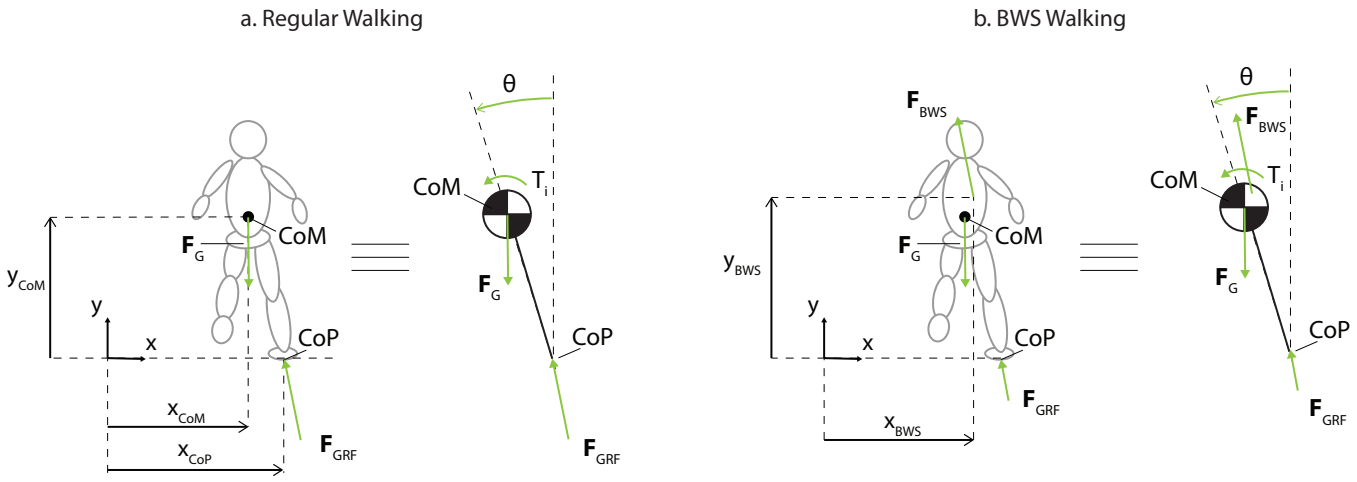

Fig. 2. Free-body diagrams of a walking human in the single-stance phase seen in the frontal plane. The figure on the left shows the forces acting on the body during regular walking. The figure on the right shows an added BWS force acting on the upper body.

From now on, $\frac{I_{\text{CoM}}}{m y_{\text{CoM}}} + y_{\text{CoM}}$ will be named the equivalent length l_{eq}. Combining Eq. (1) and Eq. (5) shows two distinct mechanisms to control the mediolateral CoM acceleration

$$m \cdot \ddot{x}_{\text{CoM}} = F_{\text{GRF}x} = \underbrace{-\frac{x_{\text{CoP}} - x_{\text{CoM}}}{l_{\text{eq}}} \cdot F_{\text{GRF}y}}_{\text{CoP displacement}} - \underbrace{\frac{T_{\text{i}}}{l_{\text{eq}}}}_{\text{counter rotation}}. \tag{6}$$

The CoP-displacement term shows the coupling between $F_{\text{GRF}x}$ and $F_{\text{GRF}y}$. During walking, humans control the CoP displacement with respect to the CoM with the foot-placement and ankle strategy. In product with $F_{\text{GRF}y}$, this creates a component of $F_{\text{GRF}x}$, which results in an ML acceleration of the CoM. The counter-rotation term illustrates how the counter-rotation strategy results in an opposing force through the ground reaction force. Fig. 3 illustrates the position and orientation of the $\boldsymbol{F}_{\text{GRF}}$ in the frontal plane

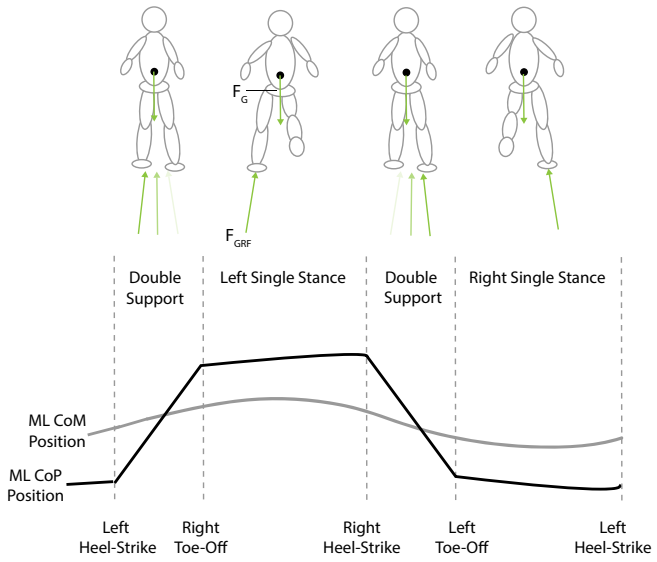

Fig. 3. One gait cycle in the frontal plane. The ML CoM and CoP position are plotted as a function of the gait phase. The illustrations above the graph show how the direction of the $\boldsymbol{F}_{\text{GRF}}$ changes through-out the gait cycle.

during walking and the ML movement of the CoM. Humans walk with a step width, which means that there is an ML distance between the CoM and CoP. Due to this distance, an ML component of the $\boldsymbol{F}_{\text{GRF}}$ develops, which accelerates the CoM in the ML direction. In each subsequent step, the direction of this acceleration changes, which results in an oscillating movement of the CoM.

Fig. 2b shows the free-body diagram when a BWS force ($\boldsymbol{F}_{\text{BWS}}$) is acting on the upper body. When this force is introduced, the force balances change to

$$\sum F_x = m\ddot{x}_{\text{CoM}} = F_{\text{GRF}x} + F_{\text{BWS}x} \tag{7}$$

$$\sum F_y = m\ddot{y}_{\text{CoM}} = F_{\text{GRF}y} - mg + F_{\text{BWS}y}. \tag{8}$$

When we compare Eq. (7) to Eq. (1), we see that the ML acceleration of the CoM is now influenced both by the $F_{\text{GRF}x}$ and the $F_{\text{BWS}x}$. Comparing Eq. (8) to Eq. (2), it becomes apparent that the vertical BWS force ($F_{\text{BWS}y}$) decreases the magnitude of the $F_{\text{GRF}y}$. The moment balance around the CoM changes to

$$\begin{aligned}\sum M_{\text{CoM}} =& I_{\text{CoM}} \cdot \ddot{\theta} \\ =& y_{\text{CoM}} \cdot F_{\text{GRF}x} + (x_{\text{CoP}} - x_{\text{CoM}}) \cdot F_{\text{GRF}y} + T_{\text{i}} \\ &+ (x_{\text{BWS}} - x_{\text{CoM}}) \cdot F_{\text{BWS}y} \\ &- (y_{\text{BWS}} - y_{\text{CoM}}) \cdot F_{\text{BWS}x}.\end{aligned} \tag{9}$$

Using the same substitutions and assumptions as Eq. (6), the following expression for the ML acceleration of the CoM is obtained as

$$\begin{aligned}m\ddot{x}_{\text{CoM}} =& F_{\text{GRF}x} + F_{\text{BWS}x} \\ =& \underbrace{-\frac{x_{\text{CoP}} - x_{\text{CoM}}}{l_{\text{eq}}} \cdot F_{\text{GRF}y}}_{\text{CoP displacement}} - \underbrace{\frac{T_{\text{i}}}{l_{\text{eq}}}}_{\text{counter rotation}} \\ &\underbrace{-\frac{x_{\text{BWS}} - x_{\text{CoM}}}{l_{\text{eq}}} \cdot F_{\text{BWS}y}}_{\text{lateral alignment}} + \underbrace{\frac{y_{\text{BWS}}}{l_{\text{eq}}} \cdot F_{\text{BWS}x}}_{\text{lateral support}}.\end{aligned} \tag{10}$$

Compared to Eq. (6), which showed a human walking without BWS, several things have changed in Eq. (10). Because the $F_{\mathrm{GRF}y}$ decreases in the presence of the $F_{\mathrm{BWS}y}$, the CoP-displacement term is affected – for the same distance between the CoP and CoM, an increase in the $F_{\mathrm{BWS}y}$ decreases its magnitude. This relates to our hypothesis that the step width will increase when vertical unloading rises: the increased step width compensates for the decreased $F_{\mathrm{GRF}y}$. Because an increased step width increases the energetic losses due to impact during walking, we further hypothesized that alternative balancing strategies would be recruited more. An increased use of the ankle strategy would cause the CoP trajectory under the foot to move more laterally during the single stance phase. Furthermore, the counter-rotation term appears to be unaffected by the $\boldsymbol{F}_{\mathrm{BWS}}$, which motivates our hypothesis that the counter-rotation strategy will be used more when the vertical unloading increases. The lateral-alignment term shows that an ML distance between the point of application of the $\boldsymbol{F}_{\mathrm{BWS}}$ and the CoM creates a moment around the CoM, which is balanced by an ML component of the $\boldsymbol{F}_{\mathrm{GRF}}$. The lateral-support term shows how lateral support forces influence the ML acceleration of the CoM. When the $F_{\mathrm{BWS}x}$ acts as a lateral stiffness or damping, this decreases the requirement of the human to actively contribute to the ML CoM acceleration themselves.

B. Participants. Fifteen healthy participants [9 male, 6 female; age 26 ± 3 years; height 1.78 ± 0.10 m, weight 75 ± 8.6 kg (mean ± SD)] took part in the experiment. The Delft Human Research Ethics committee accepted the conduction of the experiment. Each of the participants gave written consent for their participation and the use of their data for this thesis. A copy of the consent form can be found in Appendix A.

C. Instrumentation. The experiments have been conducted in the BioMechaMotion Lab at the faculty of Mechanical, Maritime and Materials Engineering (3mE) at Delft University of Technology. The measurement equipment consisted of a 12 camera motion capture system (Qualisys, Götenburg, Sweden) and two force plates (Kistler B.V., Eemnes, The Netherlands). An 8 meter long walkway was placed across the length of the laboratory with the two force plates located in the middle. Appendix B Fig. A1 shows a visualisation of the walkway.

The RYSEN BWS system was used to induce the experimental conditions. Fig. 4 shows a render of the system. Cables are attached to a harness worn by the participant. These cables provide BWS and the suspension point tracks the individual through the workspace. Apart from vertical unloading, the device also enables the generation of lateral forces.

D. Conditions. There were a total of 7 experimental conditions, listed in Table 2. The first condition consisted of regular walking (RW) without being attached to the RYSEN. In three conditions (20G, 40G, 60G), a vertical unloading of 20%, 40% and 60% of the BW was provided while keeping the device in its laterally guided suspension mode.

In two conditions ($\mathrm{K_L}$, $\mathrm{K_H}$), the RYSEN was used to simulate the spring-like laterally stabilizing forces of a LF BWS system. Fig. 1a visualizes how $F_{\mathrm{GRF}x}$ develops in a LF BWS system. For this force, the following geometric relation holds:

$$\frac{F_{\mathrm{BWS}x}}{F_{\mathrm{BWS}y}} = \frac{x_{\mathrm{SP}} - x_{\mathrm{BWS}}}{y_{\mathrm{SP}} - y_{\mathrm{BWS}}}, \tag{11}$$

which means that the lateral force is equal to

$$F_{\mathrm{BWS}x} = \frac{F_{\mathrm{BWS}y}}{y_{\mathrm{SP}} - y_{\mathrm{BWS}}} \cdot (x_{\mathrm{SP}} - x_{\mathrm{BWS}}). \tag{12}$$

This is similar to the force equation for a spring, where in this case the spring stiffness is equal to $\frac{F_{\mathrm{BWS}y}}{y_{\mathrm{SP}} - y_{\mathrm{BWS}}}$. The stiffness is proportional to the vertical unloading and inversely proportional to the height difference between the point of application of the $\boldsymbol{F}_{\mathrm{BWS}}$ and the suspension point. In the $\mathrm{K_L}$ and $\mathrm{K_H}$ conditions, a LF BWS sytem with suspension point height ($y_{\mathrm{SP}} - y_{\mathrm{BWS}}$) of 5 m and 2 m were simulated,

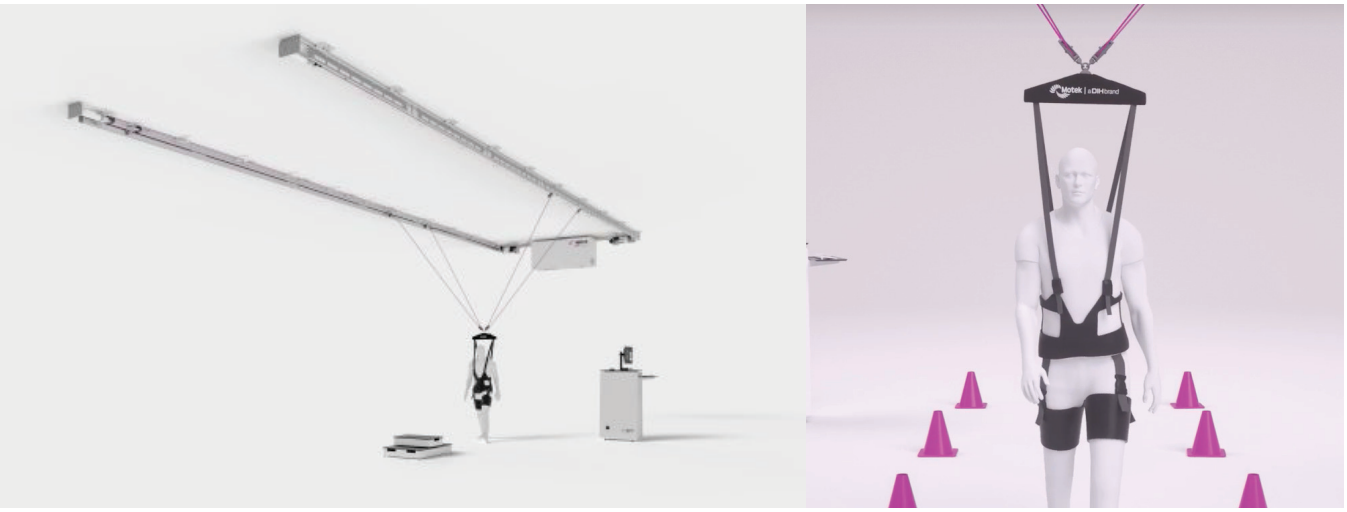

Fig. 4. The RYSEN Overground Bodyweight Support system. The suspension point tracks the user, who can walk freely within the bounds of the system without being constrained to the path of a guiding rail. In the right picture, a close-up of the user in the frontal plane wearing the support harness is shown.

Table 2. Experimental conditions.

Condition	$F_{\mathrm{BWS}y}$	Lateral Support
RW	None	None
20G	20% BW	Guided Suspension
40G	40% BW	Guided Suspension
60G	60% BW	Guided Suspension
K_L	40% BW	Low Stiffness: 8% BW/m
K_H	40% BW	High Stiffness: 20% BW/m
D	40% BW	Damping: 75 Nm/s

resulting in respectively a high (20% BW/m) and low (8% BW/m) stiffness. In the last condition (D) a damping of 75 Ns/m is applied.

E. Protocol. The participants were asked to wear tight-fitting sporting clothes and perform the walking trials with bare feet. They were outfitted with the RYSEN harness, after which their height and weight were measured. Twenty reflective markers were placed on the lower extremity, Appendix C shows pictures of a participant wearing the marker set. Because the RYSEN harness is worn over the anatomical landmarks of the pelvis, the reflective markers for the pelvis were placed on the harness.

Participants walked at a comfortable self-selected walking speed and cadence with their arms free. A total of 20 succesful walkway passes were recorded per condition, succes defined by a full hit of the feet on both of the force plates. To prevent participants attempting to step conciously on the force plates in the walkway, they were instructed to focus their gaze on a picture placed at eye-level on the opposite end of the walkway.

The rest of the conditions provided different levels of $\boldsymbol{F}_{\mathrm{BWS}}$ and lateral support, as shown in Table 2. The order of the conditions was determined by using a balanced Latin square (Campbell and Geller (1980)).

F. Data Analysis. Custom scripts in Matlab (Mathworks, Natick, USA) were used to analyze the data. Initial contact and toe-off events were detected with thresholds on the vertical force plate data and by using the algorithm of Zeni et al. (2008). For each walkway pass, two strides were collected for further analysis, of which one stride collected force plate data for each step (FP Stride) and one stride without any force data. Fig. 5 provides a visualisation of the outcome measures described in this section.

Step width was computed from the ML distance between the left and right ankle joint in the middle of double support for both of the extracted strides. Appendix D shows how the ankle joint position is calculated from the motion capture markers. Step width variability was computed as the standard deviation of all step width measures in the same condition. The use of the ankle strategy was operationalized by the CoP Shift parameter (Hof et al. (2010)). It is defined as the mean lateral distance of the CoP with respect to its initial position during single stance.

The CoM position was estimated as the mean position of the four pelvis markers. To determine the CoM kinematics, a sinusoid was fitted (SineFit function, Matlab Exchange) on the ML CoM position for the FP Stride. The CoM displacement was defined as the peak-to-peak distance of the sinusoid function. The CoM Velocity was computed as the maximum value of the differentiated sinusoid function. The XCoM was computed as $\mathrm{XCoM} = x_{\mathrm{CoM}} + \sqrt{\frac{y_{\mathrm{CoM}}}{g}} \cdot \dot{x}_{\mathrm{CoM}}$ (Hof et al. (2005)). The CoM height y_{CoM} was assumed to be constant during the gait cycle and estimated from anthropometric tables as 55% of the total body height (Winter (2009)). The effective gravitational constant g was scaled with the provided BWS force. The base of support was defined by the definition of Hof et al. (2005) as the distance between the minimum and maximum CoP location during a single stride. The margin of stability was computed as an average over two steps, by subtracting the peak-to-peak distance of the XCoM from the base of support of the same FP Stride and dividing by 2.

Eq. (10) shows the contribution of the CoP displacement, counter rotation, and the point of application of the $\boldsymbol{F}_{\mathrm{BWS}}$ on the ML acceleration of the CoM. To assess the relative use of the counter-rotation strategy, the $F_{\mathrm{GRF}x}$ is further analyzed. From Eq. (10) we see that the $F_{\mathrm{GRF}x}$ is built up as follows:

$$F_{\mathrm{GRF}x} = \underbrace{-\frac{x_{\mathrm{CoP}} - x_{\mathrm{CoM}}}{l_{\mathrm{eq}}} \cdot F_{\mathrm{GRF}y}}_{\text{CoP displacement}} \underbrace{-\frac{T_{\mathrm{i}}}{l_{\mathrm{eq}}}}_{\text{counter rotation}} \underbrace{-\frac{x_{\mathrm{BWS}} - x_{\mathrm{CoM}}}{l_{\mathrm{eq}}} \cdot F_{\mathrm{BWS}y}}_{\text{lateral alignment}} \underbrace{+\frac{y_{\mathrm{BWS}} - l_{\mathrm{eq}}}{l_{\mathrm{eq}}} \cdot F_{\mathrm{BWS}x}}_{\text{lateral support}}. \tag{13}$$

When walking in a BWS system, care is taken that users wear the BWS harness as symmetrically as possible. Therefore, it was assumed that the BWS force is aligned with the ML position of the CoM, which eliminates the lateral-alignment term. For frontal plane movement, when h is defined as the height of the trochanter joint, l_{eq} can be approximated as $1.34h$ and y_{CoM} can be approximated as $1.10h$ (Kodde et al. (1979)). This means that l_{eq} is approximately 20% larger than the CoM. The RYSEN harness is worn on the pelvis, so that y_{BWS} is kept intentionally higher than y_{CoM}. If $y_{\mathrm{BWS}} < y_{\mathrm{CoM}}$, $\boldsymbol{F}_g$ and the $\boldsymbol{F}_{\mathrm{BWS}}$ would create a destablizing force couple and the person could flip over and get injured. Therefore, the vertical point of application of the BWS is assumed to be somewhere between the CoM and l_{eq}, which means that the difference between y_{BWS} and l_{eq} is relatively small. Furthermore, $F_{\mathrm{BWS}x}$ should be close to zero when guided unloading is provided. Therefore, it becomes plausible to also eliminate the lateral-support term from the equation. Eliminating the lateral-alignment and lateral-support terms leaves

$$\underbrace{F_{\mathrm{GRF}x}}_{F_{\mathrm{GRF}x:\mathrm{Total}}} = \underbrace{\frac{x_{\mathrm{CoP}} - x_{\mathrm{CoM}}}{l_{\mathrm{eq}}} F_{\mathrm{GRF}y}}_{F_{\mathrm{GRF}x:\mathrm{CoP}}} + \underbrace{\frac{T_{\mathrm{i}}}{l_{\mathrm{eq}}}}_{F_{\mathrm{GRF}x:\mathrm{CR}}}. \tag{14}$$

During the experiments, the $F_{\mathrm{GRF}x:\mathrm{Total}}$ is measured by the force plates. The $F_{\mathrm{GRF}x:\mathrm{CoP}}$ component can be estimated

with the measurements of x_{CoP}, x_{CoM} and $F_{\text{GRF}y}$ and the assumed $l_{\text{eq}} = 1.34h$.

It is then possible to compare the measured total $F_{\text{GRF}x}$ to the estimated CoP-displacement component of the $F_{\text{GRF}x}$. This is done similar to Herr and Popovic (2008) by using the coefficient of determination (R^2), which is computed as

$$R^2 = 1 - \frac{\text{var}\left(\boldsymbol{F}_{\text{GRF:CoP}} - \boldsymbol{F}_{\text{GRF}x\text{:Total}}\right)}{\text{var}\left(\boldsymbol{F}_{\text{GRF}x\text{:Total}}\right)}. \qquad \textbf{(15)}$$

where $\boldsymbol{F}_{\text{GRF}x\text{:CoP}}$ is a timeseries of the CoP-displacement component of the $F_{\text{GRF}x}$ and $\boldsymbol{F}_{\text{GRF}x\text{:Total}}$ a timeseries of the total measured $F_{\text{GRF}x}$. The timeseries start when the leading foot is in contact with the first force plate of the walkway right after toe-off of the trailing leg, and ends just before heelstrike with the walkway after the second force plate. Only during this time period the feet are only in contact with the force plates and the CoP location and the $\boldsymbol{F}_{\text{GRF}}$ can be fully determined.

A decreased R^2 would reflect that the variance of $\boldsymbol{F}_{\text{GRF}x\text{:Total}}$ is to a lesser extent caused by the CoP-displacement mechanism. When the assumptions leading to Eq. (14) hold, this would indicate that the counter-rotation strategy is recruited relatively more to control lateral balance.

To illustrate, Appendix E Fig. A7 shows a plot of the measured $F_{\text{GRF}x}$ and the CoP-Displacement component of the $F_{\text{GRF}x}$ for one walkway pass of one participant in the RW condition. The difference in shape between the $\boldsymbol{F}_{\text{GRF}x\text{:Total}}$ and $\boldsymbol{F}_{\text{GRF}x\text{:CoP}}$ plot may then be attributed to the contribution of the counter-rotation strategy to the $F_{\text{GRF}x}$ or modeling errors.

G. Statistical Analysis. The data was first assessed for their validity of using parametric statistical tests (repeated measures ANOVA, dependent t-test). However, there were outliers present in the data of all the outcome measures which would bias these tests. Therefore, non-parametric statistical tests were used. Friedman's ANOVA test was used to test for the main effect. The difference between the conditions and the baseline was determined by using Wilcoxon signed-rank tests. To compensate for a possible inflation of type II errors, a Bonferonni correction was used. Therefore, all of the reported outcome measures are only accepted as significant when $p < 0.05/3 = 0.017$.

Two separate Friedman's ANOVA analyses were performed for each of the outcome measures. The first analysis tested the influence of vertical unloading. Wilcoxon signed-rank tests were performed that compared the 20G, 40G, and 60G conditions to the to the RW condition. The second analysis tested the effect of different lateral support conditions at 40% vertical unloading. Wilcoxon signed-rank tests compared th K_H, K_L, and D to the 40G condition.

3: Results

The effect of vertical unloading is visualized in Fig. 6 and lateral support in Fig. 7. In the boxplots presented in this article, the between-subject variance has been removed, so that the within-subject differences become more apparent from the visualisation (Loftus and Masson (1994)). This removal is further illustrated in Appendix F. In Appendix G, Table A3 and Table A4 list the statistics of the Friedman's ANOVA and Wilcoxon signed-rank tests for the effect of respectively vertical unloading and lateral support. In Appendix H an alternative visualisation of the data is shown, by plotting the relative percentual difference of the outcome measures with respect to the RW and 40G conditions.

Fig. 6a shows that individuals step slightly wider in the 60G condition (median 9% difference). In Fig. 6b we see there is no effect of vertical unloading on the step width variability. The step width variability seemed to increase in the 60G condition (median 21% difference to RW), but no significant difference was found (p = 0.031). Fig. 6c shows that R^2 decreased significantly for the 40G and 60G conditions (respectively median 6% and 21% difference). In Appendix E, Fig. A5 and Fig. A6 show density scatter plots of the $F_{\text{GRF}x\text{:CoP}}$ versus the $F_{\text{GRF}x\text{:Total}}$. In Fig. 6d it becomes apparent that the CoP did not shift more laterally due to vertical unloading. Figures 6e and 6f show that the CoM displacement and velocity decreased for both the 40G and 60G conditions (displacement: respectively median

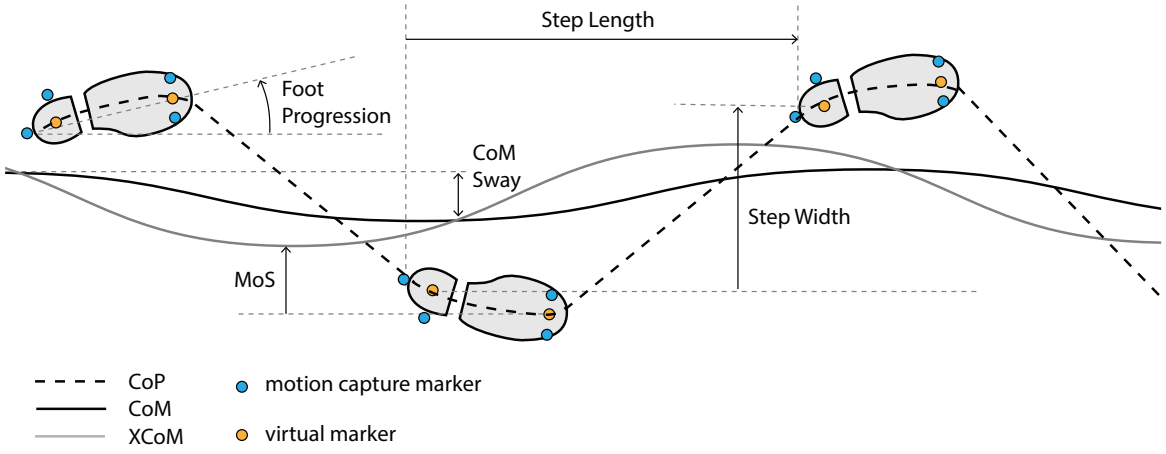

Fig. 5. Spatial definition of several of the outcome measures.

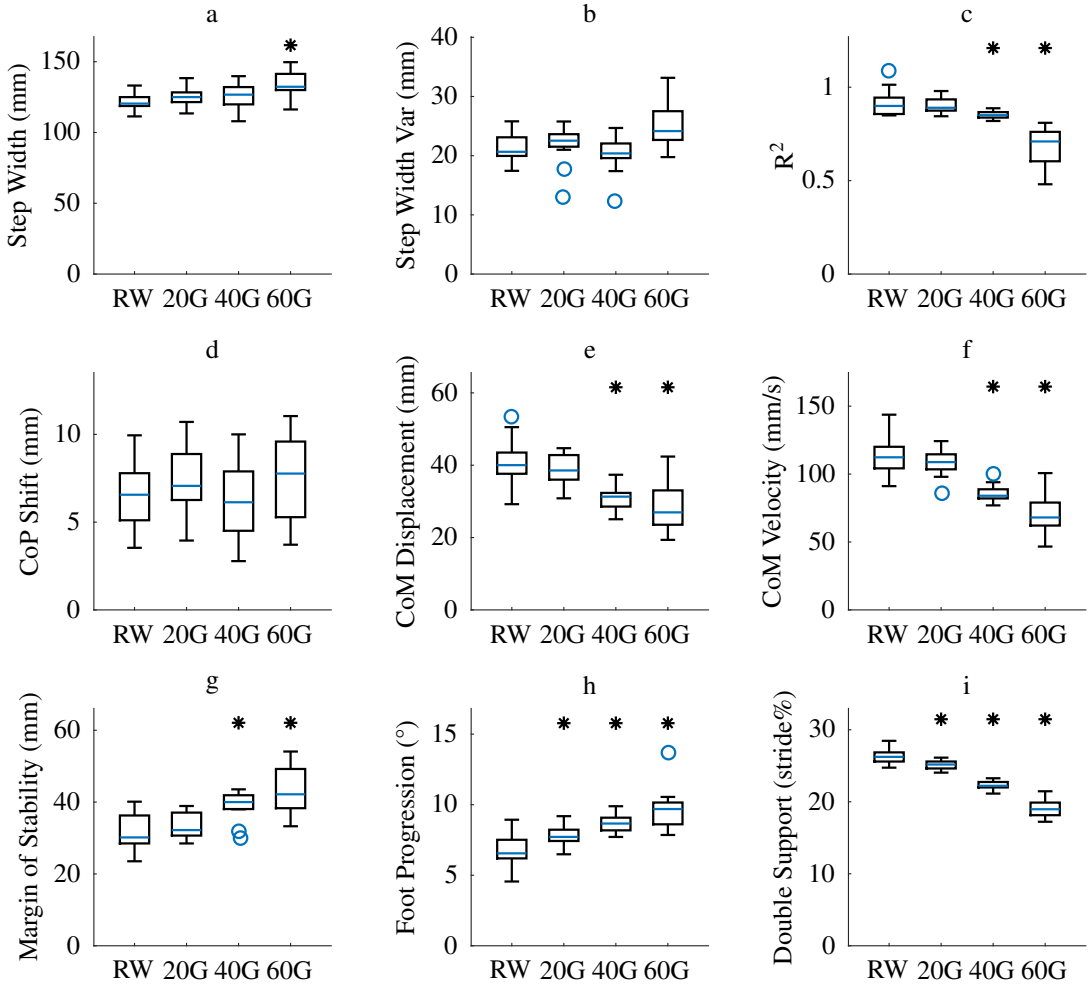

Fig. 6. Boxplots of the effect of vertical unloading on the outcome measures. The between subject variance has been removed in these plots. An asterisk (*) above the boxplot indicates a significant difference to the RW condition.

22% and 36% difference, velocity: respectively median 25% and 39% difference). The margin of stability increased for both the 40G and 60G condition (respectively median 23% and 36% difference). In Fig. 6h a significant increase of the foot progression is observed for all of the conditions (respectively median 16%, 30%, and 46% difference). Fig. 6i shows a significant decrease of the relative time spent in the double support phase when unloading increases (respectively median 4%, 16%, and 28% difference).

Fig. 7 visualizes that most of the outcome measures showed no effect of lateral support in this experiment. Fig. 7b does show a decreased step width variability for the K_L condition (median 21% difference with RW). Fig. 7f shows that the CoM velocity increased for the D condition (median 9% difference with RW).

In this experiment the walking speed and cadence were not controlled. Participants were asked to walk at a comfortable walking speed. In Appendix L, figures A20c and A20d show the walking speed and cadence in the vertical unloading conditions. For both the cadence and walking speed, only a significant difference with respect to RW was found for the 60G condition (walking speed: median 12% difference, cadence: median 7.5% difference). No significant differences were found for the lateral support conditions.

4: Discussion

A. Vertical unloading changes lateral balance related gait parameters. Apte et al. (2018) recently published a meta-analysis on the effect of BWS on a multitude of gait characteristics and showed that mostly the joint moments, muscle activity, energy cost of walking, and ground reaction forces decreased due to the unloading. Their analysis, however, only included gait parameters in the sagittal plane and did not report on the gait parameters that allude to control of lateral balance. Our experiment shows that BWS has a considerable effect on gait parameters related to lateral balance. Apte et al. (2018) noted that gait characteristics mostly seem to change when vertical unloading higher than 30% of the BW is provided. This lower bound seems to align with our results, as we only found significant effects in the 20G conditions for foot progression and double support time.

We hypothesized that step width and its variability would increase with vertical unloading. The step width did not increase as much as expected – it increased only for the 60G condition, similar to the results by Dragunas and Gordon (2016) on a LF BWS system. Because lateral stabilization

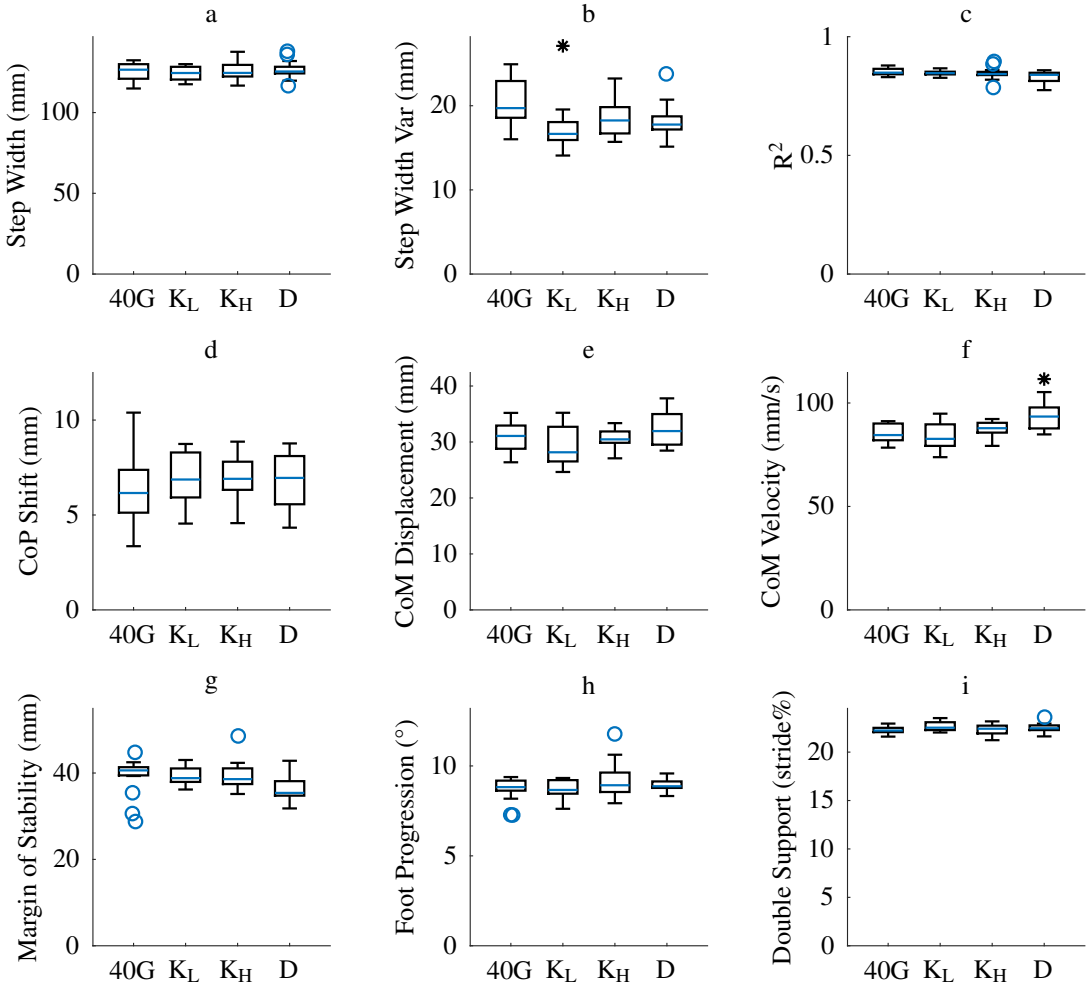

Fig. 7. Boxplots of the effect of lateral support on the outcome measures. The between subject variance has been removed in these plots. An asterisk (*) above the boxplot indicates a significant difference to the 40G condition.

usually decreases the step width, we expected a more pronounced effect of unloading on the step width in LG BWS systems compared to LF BWS. The step width variability showed no effect of vertical unloading. This unchanged step width suggests that BWS only has a minimal effect on the foot placement strategy.

There was no effect found for the CoP shift. We hypothesized that strategies other than the foot placement strategy would be recruited more when unloading increases. Increased use of the ankle strategy would have shown as a lateral shift of the CoP under the foot during the single stance phase. We observed no significant effect of vertical unloading on the CoP shift, which suggests a similar use of the ankle strategy across the vertical unloading conditions. Experiments by Fischer and Wolf (2016) do show a significant lateral shift of the CoP trajectory caused by BWS, even under relatively low unloading conditions (15% and 30% BW). However, they obtained their data from only six steps per condition, compared to the 40 steps per condition of this experiment. It could have been that their operationalization of the CoP caused an error. They computed the mean CoP location orthogonally to the midline of the foot, which means that changes in foot progression confound their results. We found a significant increase in the foot progression for each of the vertical unloading conditions, which might explain the contradicting results for the lateral CoP shift.

Both the CoM displacement and velocity decreased significantly for the 40G and 60G condition. This decrease might be explained by evaluating the equations of motion of lateral balance. Eq. (14) shows that the $F_{\mathrm{GRF}x}$ is primarily caused by the distance between the CoP and CoM – its size is relative to the ML distance of the CoP to the CoM multiplied by the $F_{\mathrm{GRF}y}$. Humans walk with a step width, so when walking is initiated from a standstill, the $F_{\mathrm{GRF}x}$ under the feet causes a medial acceleration of the CoM. Due to vertical unloading, the $F_{\mathrm{GRF}y}$ decreases, so to develop the same forces under the foot, the distance between the CoP and CoM would have to increase proportionally. In Appendix J, Fig. A15 shows the effect of BWS on the ML distance between the CoM and CoP during the single-stance phase of walking. It shows that this distance increases with unloading, but not relative to the amount of unloading (median difference 32% and 45% for the 40G and 60G condition). Therefore, fewer ML forces were developed under the feet, which caused a smaller acceleration, and

therefore velocity and displacement of the CoM. We found some further explanation in analyzing the lateral forces estimated by the RYSEN. In Appendix I, Fig. A13 shows that the RMS value of these lateral forces increases with vertical unloading. Eq. (7) shows how both the $F_{\text{GRF}x}$ and the $F_{\text{BWS}x}$ influence the acceleration of the CoM. In Appendix K, Fig. A18 shows that the $F_{\text{GRF}x}$ has a mean value of 1.8% of the BW for the 60G condition, while Appendix I Fig. A13 reveal that the RMS lateral force of the RYSEN is 0.5% in the same condition. Hence, the decreased CoM displacement and velocity can be attributed both to the decreased the $F_{\text{GRF}x}$ attributed to the CoP-displacement mechanism, and by the relatively increased influence of the $F_{\text{BWS}x}$ on the ML acceleration of the CoM when unloading increases.

B. Vertical unloading decreases the relative contribution of CoP displacement to lateral balance. The relative contribution of the CoP-displacement mechanism to the $F_{\text{GRF}x}$ seems to decrease with unloading. This is indicated by the decreased value of the R^2 parameter in the 40G and 60G condition. This parameter represents the correlation between the measured $F_{\text{GRF}x}$ and the component of the $F_{\text{GRF}x}$ attributed to the CoP-displacement mechanism. In Appendix E, density scatter plots are provided, which further visualize the correlation. When this correlation decreases, this indicates that changes in the $F_{\text{GRF}x}$ are to a lesser extent caused by the CoP-displacement mechanism.

A similar analysis of R^2 during regular walking was done by Herr and Popovic (2008), who found that its value is high (> 0.9) during regular overground walking. This value aligns with our results for the RW condition, which shows a median value of R^2 of 0.92. Furthermore, Hof (2007) used a similar outcome measure (a regression coefficient) and showed experimentally that this coefficient decreases when inertial strategies are used to control postural balance. Therefore, it is interesting that R^2 decreases significantly when humans walk in the 40G and 60G condition, as this might indicate an increase in the relative use of the counter-rotation strategy with respect to the CoP-displacement mechanism when BWS is provided.

Our results suggest a reweighing in the recruitment of the different balancing strategies when unloading is provided. The unchanged CoP Shift parameter indicates that the CoP did not move more laterally due to the ankle strategy when unloading was provided. The step width increased slightly in the 60G condition, and the step width variability showed no change. However, Appendix J Fig. A15 shows that the distance between the CoM and CoP increased for the 40G and 60G conditions. Therefore, it seems that the foot placement is used relatively more compared to the ankle strategy when unloading increases. The decrease of R^2 implies that the counter-rotation strategy is used more relative to both the foot-placement and ankle strategy when unloading increases.

The conclusion that a decreased R^2 implies increased use of the counter-rotation strategy is based on the assumptions that the $\boldsymbol{F}_{\text{BWS}}$ applies approximately at the CoM and that modeling errors are minimal. These assumptions might have biased the analysis. Eq. (13) shows the different terms that contribute to the $F_{\text{GRF}x}$. The lateral-alignment and lateral-support terms should be relatively small compared to the magnitude of the measured $F_{\text{GRF}x}$. For both to vanish completely from the equation, the point of application of the $\boldsymbol{F}_{\text{GRF}}$ should coincide laterally with the center of mass ($x_{\text{BWS}} - x_{\text{CoM}} = 0$) and vertically with the equivalent pendulum length ($y_{\text{BWS}} - l_{\text{eq}} = 0$). The equivalent length l_{eq} is assumed to remain constant, even though the CoM moves vertically across the gait cycle. The CoM location is approximated by the pelvis markers, although this gives a slight overestimation when compared to the CoM location computed from a whole-body marker set (Whittle (1997)). The effect of the impact at heelstrike on the $F_{\text{GRF}x}$ is not modeled, even though this shows as a distinct peak in the $F_{\text{GRF}x}$ at that moment in the gait cycle (see Appendix E Fig. A7).

The location where the $\boldsymbol{F}_{\text{BWS}}$ applies on the human seems to have a large contribution to the $F_{\text{GRF}x}$. During the experiments, care was taken that the support harness was worn as horizontally symmetrically as possible. However, it is unknown how the point of application may have moved during the walking gait. The support harness transmits the forces of the RYSEN to the body. Those forces are transmitted as a distributed pressure on the body over the harness and not a fixed point. The center of this pressure distribution is the equivalent point of application of the $\boldsymbol{F}_{\text{BWS}}$. In this experiment, the $F_{\text{BWS}y}$ is 20%, 40%, or 60% of the BW. When the point of application moves laterally for an arbitrarily chosen, but plausible range of $\pm 2\%$ of l_{eq}, the $F_{\text{GRF}x}$ is influenced as

$$\frac{x_{\text{BWS}} - x_{\text{CoM}}}{l_{\text{eq}}} F_{\text{BWSy}} \approx \pm 2\% \cdot (20\%, 40\%, 60\%)\text{BW}$$

which is approximately equal to $\pm 0.4\%$, $\pm 0.8\%$, and $\pm 1.2\%$ of the BW. In this experiment, the median values of the $F_{\text{GRF}x}$ for the unloading conditions were 3.5% BW for 20G, 2.7% BW for 40G, and 1.7% BW for the 60G condition (see Appendix K Fig. A18). Therefore, only a small horizontal displacement of the point of application of the $\boldsymbol{F}_{\text{BWS}}$ can have a relatively large influence on the $F_{\text{GRF}x}$.

When the vertical point of application does not coincide with the compound pendulum height l_{eq}, the $F_{\text{BWS}x}$ also starts to influence the $F_{\text{GRF}x}$. Appendix I Fig. A13 shows the RMS value of the $F_{\text{BWS}x}$ during the walking trials. Its median magnitude was 0.3% BW for 20G, 0.4% BW for 40G, and 0.5% BW for the 60G condition. This means that l_{eq} is approximately 20% higher than the CoM. The vertical point of application can reasonably be assumed to between y_{CoM} and l_{eq}. The contribution of the $F_{\text{BWS}x}$ on the $F_{\text{GRF}x}$ is therefore approximately

$$\frac{y_{\text{BWS}} - l_{\text{eq}}}{l_{\text{eq}}} F_{\text{BWS}x} \approx \frac{100\% - 120\%}{120\%} \cdot (0.3\%, 0.4\%, 0.5\%)\text{BW}$$

which is a negligibly small contribution to the $F_{\text{GRF}x}$.

When the lateral point of application of the $\boldsymbol{F}_{\text{GRF}}$ would have perfectly coincided with the CoM, the decrease

in R^2 could have been attributed to an increase in the counter-rotation strategy. However, an estimation of the relative contribution to the $F_{\mathrm{GRF}x}$ by the possibly shifting lateral point of application of the $\boldsymbol{F}_{\mathrm{BWS}}$ showed a substantial influence. Post-hoc analysis of video footage during the experiment also suggested that the lateral alignment of the $\boldsymbol{F}_{\mathrm{BWS}}$ played a substantial role. Videos of participants (P4, P5, P12) with a low value of R^2 in the 60G conditions revealed that the vertical support force was provided lateral to the COM, which caused a lateral drift of the participants towards either the left or right edge of the walkway. These video images provide further evidence that we can not attribute the decrease of R^2 to an increase in the counter-rotation strategy. However, these results do show that the lateral alignment of the $\boldsymbol{F}_{\mathrm{BWS}}$ has a substantial effect on lateral balance.

C. Vertical unloading produces a more cautious gait. The increased margin of stability and foot progression suggests that the higher unloading levels produce a more cautious gait. Most indicative of this is the margin of stability – the distance between the most lateral position of the CoP and XCoM during a step. If the margin of stability is small, a perturbation in the walking gait can cause the CoM to tip-over the stance foot and move laterally. To correct for the perturbation and remain upright, a human can use their counter-rotation strategy or perform a cross step. Cross stepping can lead to falls as the swing leg has to circumvent the stance leg, which can lead to tripping. Increasing the margin of stability decreases the likelihood that the CoM leaves the base of support during walking. In a recent article by Wu et al. (2020) the effect of lateral destabilization by a negative damping field on lateral stability was studied. They found that the MoS increased when walking in a destabilizing damping field. This increase also further substantiates the claim by Dragunas and Gordon (2016) that vertical unloading is a destabilizing force.

The foot progression increased significantly for each of the unloading conditions. A more substantial foot progression means that the human walks with their toes pointed more laterally. The more the toes are pointed laterally, the more the CoP can be moved laterally by the ankle strategy during the stance phase. However, we found no effect for the CoP shift. Even though the foot progression increased, this did not affect the lateral position of the CoP. Therefore it could be that the increased foot progression created a larger 'safety margin' for the CoP movement of the ankle strategy in anticipation of instability.

D. Lateral support showed almost no statistically significant effects. No effect of lateral stabilization was found for the step width. This contradicts the conclusion of Pennycott et al. (2011), who reasoned that the step width in their experiment decreased due to the laterally stabilizing forces of LF BWS systems. Our results show that the step width variability decreased, but only for the lateral support condition with the lowest stiffness ($\mathrm{K_L}$). We expected that a higher lateral stiffness would show an equal or larger decrease of the step width variability, but found no significant decrease for that condition. The almost absent effects on step width and its variability contrast with Donelan et al. (2004), Dean et al. (2007), IJmker et al. (2014), and Matsubara et al. (2015), who all show that that the step width and its variability decrease when a stiffness provides lateral stabilization to the pelvis. Wu et al. (2017) shows that lateral damping on the pelvis decreases the step width.

The CoM velocity increased in the lateral damping condition. Because damping exerts a force in the opposite direction of velocity, we expected that the maximum velocity would decrease. Such a result would have agreed with Wu et al. (2017), who found that lateral damping in treadmill walking decreases the CoM velocity. The contradicting result in this experiment could be explained partially by a follow-up test with the RYSEN, which showed that the damping works uni-directionally; only velocities directed outwards from the centerline of the RYSEN elicited a damping response.

We expected that step width, step width variability, and ML CoM motion would decrease due to lateral support during unloading. Springlike lateral support forces during regular walking attenuate the motion of the center of mass (Donelan et al. (2004)). Research by Hof et al. (2010) showed that humans tend to walk with a constant margin of stability. When the CoM displacement decreases due to the springlike lateral support forces, walking with a narrower step width will still account for the same margin of stability. Matsubara et al. (2015) found that humans walk with a smaller margin of stability when springlike lateral support forces are supplied. Therefore, humans seem to start trusting and relying on lateral support forces to stabilize them. This trust and reliance would have also been reflected by a decreased step width variability, as this could indicate a decreased active participation of humans in the control task of foot placement (Beauchet et al. (2009)).

All the statistically significant results that we found in this experiment conflict with articles that studied lateral stabilization independently from BWS. However, the stiffness and damping values in these articles are much higher than the ones used in this experiment. One of the goals of this experiment was to compare LF BWS to LG BWS systems. The lateral stiffnesses were chosen such that they would represent a LF BWS with a suspension point of either 2 or 5 meters above the point of application of the $\boldsymbol{F}_{\mathrm{BWS}}$ on the human. Compared to articles that study lateral stabilization independently from BWS, these are all relatively low stiffnesses. The stiffness values in this experiment ranged between 43 and 175 N/m, compared to 1700 N/m by Donelan et al. (2004) and 1200 N/m in the experiments of Dean et al. (2007). We chose the damping in this experiment as the maximum that was allowed as an input for the RYSEN, which was 75 Ns/m, while the damping of Wu et al. (2017) ranged between 350 and 500 Ns/m. While these researchers have shown that lateral support can produce an effect on parameters related to lateral balance, our results indicate that these effects are negligible in LF BWS systems.

E. Lateral support conditions were not substantially different. The lack of effects on step width, step width variability, and CoM displacement due to lateral support could also indicate that the experimental conditions were not perfectly rendered. The RYSEN BWS device could have either not been able to simulate the provided stiffnesses and dampings, or its LG mode still produced considerable lateral forces. After conducting the experiments, we received documentation that showed the results of a parameter estimation analysis on the LG mode of the RYSEN. In this analysis, a mass-spring-damper model was fitted on the lateral motion of the RYSEN. The results showed that the residual lateral impedance of the LG mode is still substantial, with a stiffness of 116 N/m, damping of 64 Ns/m, and a mass of 2.2 kg. The lateral stiffness values used in these experiments ranged between 43 and 70 N/m for K_L and between 109 and 175 N/m for K_H, values that are quite close to the residual impedance. It is still unclear how the mass-spring-damper model fitted impedance of the RYSEN changes with different inputs for the lateral stiffness and damping. The RYSEN still provided the opportunity to tune the lateral support mode, which qualitatively seemed to have a positive effect on how participants perceived the BWS during walking. Several participants noted that walking seemed easier in the lateral support conditions. Even though this qualitative effect seemed present, the subtle differences in lateral balance that were previously reported in the literature were not replicated.

The RYSEN provides an estimated lateral force as an output. We collected this estimated lateral force for all of the experimental trials. Appendix I Fig. A13 shows boxplots of the RMS lateral force in each of the conditions. Most notably, the RMS lateral force of the LG mode increases with unloading. This increase counters the assumption of this experiment that the LG BWS allows the independent assessment of vertical and lateral forces. Wilcoxon signed-rank tests confirm that the RMS lateral force is significantly different between all of the vertical unloading conditions - the lateral forces increase when more vertical support is provided. However, the differences are only small (0.1%BW difference between the conditions). The lateral support conditions also had a different RMS lateral force for each of the conditions. Wilcoxon signed-rank tests show that all conditions are significantly different except for the RW-K_L pair.

F. Literature suggests a different effect on lateral balance by laterally-fixed suspension BWS. We noted in our research goal that assessing the influence of BWS on lateral balance from literature is difficult because mostly LF BWS systems are used. These BWS systems produce both vertical unloading and lateral restoring forces, which seem to have opposite effects on lateral balance. This experiment aimed to assess the influence of vertical and lateral forces independently but was unable to find any sensible effects for the lateral support forces. However, in this experiment, we investigated the effect of a simulated LF BWS system on lateral balance instead of an actual system. The simulated system may not have been able to provide a reliable representation of a true LF BWS system, which may explain the practically absent results. Therefore, to conclude anything about the different effects of LG and LF BWS on lateral balance, only comparisons with existing literature can be made.

The design of our experiment is most similar to that of Dragunas and Gordon (2016). The same vertical unloading conditions were provided (20%, 40%, and 60% of the BW), with the difference that we studied overground walking and used a LG BWS system. The effect of unloading on step width was similar – the step width only increased in the condition with 60% of the BW unloaded. In our experiment, the step width variability showed no effect of vertical unloading. This contrasts with Dragunas and Gordon (2016), whose results show that the step width variability decreased for 20%, 40%, and 60% of the BW unloaded. They hypothesized that this decrease was mainly due to the lateral restoring forces. They computed that the lateral restoring forces had a mean of respectively 0.4%, 0.8%, and 1.2% of the BW in the 20%, 40%, and 60% conditions. The RMS lateral forces of the LG BWS system used in this experiment were approximately 0.3%, 0.4%, and 0.5% of the BW in the ascending unloading conditions, which is considerably lower than the forces reported by Dragunas and Gordon. Beauchet et al. (2009) note that low variability in motor control reflect tasks that have minimal attention, while high variability relates to major attention involvement. Dean et al. (2007) hypothesized that an increased step width variability in older individuals is caused by decreased sensing capabilities that may introduce noise into the feedback control of the foot placement. Because lateral support forces provide extra haptic feedback on the CoM position, this might explain the decreased step width variability in those systems. The non-affected step width variability in this experiment suggests that the LG BWS has less influence on the foot-placement strategy than LF BWS systems.

In our experiment, the margin of stability increased significantly in the 40% and 60% of the BW unloading conditions, while Dragunas and Gordon (2016) found no statistically significant effect. Matsubara et al. studied the effect of a lateral stiffness on lateral stabilization, and found that the stiffness decreases the margin of stability. These results may indicate that the vertical unloading and lateral restoring forces have an opposite effect on the margin of stability, which seems to balance out in the LF BWS systems.

G. Experimental setup may have influenced the outcomes. There were multiple indications that the experimental setup could have influenced the outcomes. A Motek employee noted after the experiments that one of the bearings in the RYSEN did not work as intended. This faulty bearing could have decreased the tracking performance of the RYSEN, which would have increased the horizontal impedance of the RYSEN and created a lateral misalignment of $\boldsymbol{F}_{\text{BWS}}$ with the CoM.

During the familiarization phase of the experiment, the participants had to walk in each of the experimental

conditions until they reached a visually steady walking pattern. The participants did not always reach this visually steady pattern for the 60G condition. The condition was experienced as unpleasant by many of the participants, so it did not seem appropriate to expose them to the high unloading condition for too long. This insufficient familiarization does mean that their walking gait might have been more variable during the 60G trial, which decreases the reliability of the computed outcome measures in that condition.

Most participants noted discomfort by the RYSEN harness during the higher unloading conditions. This discomfort was mainly caused by the support force being transmitted to the body through the leg straps. The center of this pressure distribution was mainly felt in the inner thighs, which was experienced as unpleasant. In addition, this force on the inner thighs created an abduction moment around the hip joint, which could have influenced the walking pattern of the participants, most notably the lateral foot placement.

Since the experiments were conducted overground, participants could only take a limited number of steps until they reached the physical boundaries of the lab and RYSEN. In Appendix B we compared the values of the step width and step length outcome measures between the stepping locations, which show a significant difference between the steps for both parameters. This difference implies that the participants did not reach steady-state walking in this experiment.

The participants had to walk over a walkway with the force plates located in the middle. The participants could not step laterally to the force plates. Analyzing the video data of the experiment shows participants that were drifting laterally in the higher unloading conditions, but were unable to make a corrective lateral step. The force plates are narrow and could have influenced the lateral stepping of the participants.

We instructed participants to look at a picture located at eye-level at the other side of the walkway to avoid them stepping consciously on the force plates. We observed that some participants took noticeably longer or shorter steps when stepping on the first force plate in the walkway. When we observed this behavior, those trials were removed from the analysis, but more undetected trials could have occurred. According to McAndrew Young and Dingwell (2012), voluntary changes in the step length influence the computation of the margin of stability.

Only the lower extremities were outfitted with markers for the motion capture system. Therefore, the whole-body CoM was estimated from the four markers placed on the pelvis. This estimation does not provide a completely reliable estimate of the whole-body CoM position. Whittle (1997) showed that the whole-body CoM has a smaller displacement than the CoM computed from the center of the pelvis and that they are also slightly out of phase. The CoM estimation computed from the pelvis location does not take the motion of the upper-body into account. More presence of the counter-rotation strategy would imply a larger difference between the actual whole-body CoM and the one estimated from the pelvis location.

H. Recommendations. These experiments were able to make some observations regarding the difference between vertical and lateral BWS forces, but uncertainty still remains. The uncertainty was primarily caused by the fact that the RYSEN was not able to simulate these two conditions correctly. The LG mode had a residual impedance, which might have been caused by a faulty bearing in the device during the experiments. The simulated lateral support conditions were either not correctly represented by the RYSEN, or close to the residual impedance of the LG mode. Follow-up experiments should compare the effect on lateral balance by the RYSEN with an actual LF BWS system. We originally planned this comparison for the experiments described in this thesis, but the LF BWS system was not yet ready when the experiments were conducted.

The RYSEN is primarily a rehabilitation device, and not necessarily a high-fidelity haptic interface. However, its use in research could be improved by performing residual impedance analyses for different settings of the lateral stiffness and damping. This investigation would empower the use of the RYSEN as a research tool. Up until now, this analysis has only been performed on the LG mode of the device.

Analysis of the equations of motion of a walking human in BWS suggests that the contribution of the CoP-displacement mechanism to $F_{\mathrm{GRF}x}$ decreases when BWS increases. Initially, we thought that we could explain this decrease by the increased use of the counter-rotation strategy. However, the same equations of motion show a substantial possible contribution to $F_{\mathrm{GRF}x}$ due to the point of application of $\boldsymbol{F}_{\mathrm{BWS}}$. It would be beneficial to study how this point of application moves while walking in the RYSEN and how it is affected by the harness. By using a full-body marker set or IMU sensors on the upper body segments, the counter-rotation strategy could be quantified more reliably.

The analysis of lateral balance in this thesis was limited to the control of the linear CoM position. However, lateral balance also consists of controlling the angular momentum. By modeling the walking human as an inverted pendulum, one assumes that the linear CoM momentum and angular momentum around the CoM are directly coupled. The human body, however, is a multi-segmented system, for which this relation does not necessarily hold.

5: Conclusion

Increasing the vertical unloading force attenuated the mediolateral CoM motion, increased the step width, and decreased the relative time spent in the double support phase. People seemed to walk more cautiously, indicated by an increased margin of stability and foot progression angle. The relative use of different balance strategies seemed to change. Foot placement was used more relative to the ankle strategy. An analysis based on the equations of motion of human walking suggested that both the foot placement and ankle strategy had a smaller contribution to the mediolateral

ground reaction force, which implied an increased use of the counter-rotation strategy. However, the equations of motion and video footage also showed that a lateral misalignment of the BWS force with the CoM might have largely biased this analysis. Follow-up experiments should more explicitly estimate the contribution of the counter-rotation strategy to lateral balance.

This experiment aimed to study the effects of vertical unloading and lateral support during BWS independently. This goal was not reached completely. The RYSEN BWS system was used to simulate a BWS system with a fixed suspension point. This simulated system, however, seemed to produce only slightly different lateral support forces when compared to the guided suspension mode of the RYSEN. By only analyzing the current experimental data, no clear difference between guided suspension and fixed suspension BWS systems was found. Comparing our results to existing literature indicates that guided suspension has a different effect on lateral balance than fixed suspension systems. When walking in a guided suspension BWS system, the step width variability does not decrease due to unloading, while it does in previously reported experiments with a fixed suspension BWS system. This suggests that unloading in a laterally guided suspension system causes a more active control of foot placement during walking, which may be beneficial in a rehabilitation setting.

Bibliography

1. Aaslund, M. K. and Moe-Nilssen, R. (2008). Treadmill walking with body weight support. Effect of treadmill, harness and body weight support systems. *Gait Posture*, 28(2):303–308.
2. Apte, S., Plooij, M., and Vallery, H. (2018). Influence of body weight unloading on human gait characteristics: A systematic review.
3. Barbeau, H. and Fung, J. (2001). The role of rehabilitation in the recovery of walking in the neurological population. *Curr. Opin. Neurol.*, 14(6):735–740.
4. Beauchet, O., Allali, G., Annweiler, C., Bridenbaugh, S., Assal, F., Kressig, R. W., and Herrmann, F. R. (2009). Gait variability among healthy adults: Low and high stride-to-stride variability are both a reflection of gait stability. *Gerontology*, 55(6):702–706.
5. Bruijn, S., Meijer, O., Beek, P., and Van Dieën, J. (2013). Assessing the stability of human locomotion: a review of current measures. *Journal of the Royal Society Interface*, 10(83):20120999.
6. Campbell, G. and Geller, S. (1980). Balanced latin squares. *Purdue University Department of Statistics Mimeoseries*, 80(26):3–1.
7. Dean, J. C., Alexander, N. B., and Kuo, A. D. (2007). The effect of lateral stabilization on walking in young and old adults. *IEEE Trans. Biomed. Eng.*, 54(11):1919–1926.
8. Donelan, J. M., Kram, R., and Kuo, A. D. (2001). Mechanical and metabolic determinants of the preferred step width in human walking.
9. Donelan, J. M., Kram, R., and Kuo, A. D. (2002). Mechanical work for step-to-step transitions is a major determinant of the metabolic cost of human walking. *J. Exp. Biol.*, 205(Pt 23):3717–27.
10. Donelan, J. M., Shipman, D. W., Kram, R., and Kuo, A. D. (2004). Mechanical and metabolic requirements for active lateral stabilization in human walking. *J. Biomech.*, 37(6):827–835.
11. Dragunas, A. C. and Gordon, K. E. (2016). Body weight support impacts lateral stability during treadmill walking.
12. Easthope, C. S., Traini, L. R., Awai, L., Franz, M., Rauter, G., Curt, A., and Bolliger, M. (2018). Overground walking patterns after chronic incomplete spinal cord injury show distinct response patterns to unloading. *J. Neuroeng. Rehabil.*, 15(1):102.
13. Fischer, A. G. and Wolf, A. (2016). Body weight unloading modifications on frontal plane joint moments, impulses and Center of Pressure during overground gait. *Clin. Biomech.*, 39:77–83.
14. Herr, H. and Popovic, M. (2008). Angular momentum in human walking. *J. Exp. Biol.*, 211(4):467–481.
15. Hesse, S. (2008). Treadmill training with partial body weight support after stroke: A review. *NeuroRehabilitation*, 23(1):55–65.
16. Hilliard, M. J., Martinez, K. M., Janssen, I., Edwards, B., Mille, M. L., Zhang, Y., and Rogers, M. W. (2008). Lateral Balance Factors Predict Future Falls in Community-Living Older Adults. *Arch. Phys. Med. Rehabil.*, 89(9):1708–1713.
17. Hof, A. L. (2007). The equations of motion for a standing human reveal three mechanisms for balance. *J. Biomech.*, 40(2):451–457.
18. Hof, A. L., Gazendam, M. G., and Sinke, W. E. (2005). The condition for dynamic stability. *J. Biomech.*, 38(1):1–8.
19. Hof, A. L., Vermerris, S. M., and Gjaltema, W. A. (2010). Balance responses to lateral perturbations in human treadmill walking. *J. Exp. Biol.*, 213(15):2655–2664.
20. Horak, F. B. and Nashner, L. M. (1986). Central programming of postural movements: Adaptation to altered support-surface configurations. *J. Neurophysiol.*, 55(6):1369–1381.
21. IJmker, T., Noten, S., Lamoth, C. J., Beek, P. J., van der Woude, L. H., and Houdijk, H. (2014). Can external lateral stabilization reduce the energy cost of walking in persons with a lower limb amputation? *Gait Posture*, 40(4):616–621.
22. Kodde, L., Geursen, J. B., Venema, E. P., and Massen, C. H. (1979). A critique on stabilograms. *J. Biomed. Eng.*, 1(2):123–124.
23. Kuo, A. D. (1999). Stabilization of Lateral Motion in Passive Dynamic Walking. Technical report.
24. Langhorne, P., Coupar, F., and Pollock, A. (2009). Motor recovery after stroke: a systematic review. *Lancet Neurol.*, 8(8):741–754.
25. Loftus, G. R. and Masson, M. E. J. (1994). Using confidence intervals in within-subject designs. Technical Report 4.
26. MacGeer, T. (1990). Passive Dynamic Walking. *Int. J. Rob. Res.*, 9(2):62–82.
27. Mackinnon, C. D. and Winter, D. A. (1993). CONTROL OF WHOLE BODY BALANCE IN THE FRONTAL PLANE DURING HUMAN WALKING. Technical Report 6.
28. Matsubara, J. H., Wu, M., and Gordon, K. E. (2015). Metabolic cost of lateral stabilization during walking in people with incomplete spinal cord injury.
29. McAndrew Young, P. M. and Dingwell, J. B. (2012). Voluntary changes in step width and step length during human walking affect dynamic margins of stability. *Gait Posture*, 36(2):219–224.
30. Miller, C. A., Hayes, D. M., Dye, K., Johnson, C., and Meyers, J. (2012). Using the nintendowii fit and bodyweight support to improve aerobic capacity, balance, gait ability, and fear of falling: Two case reports. *J. Geriatr. Phys. Ther.*, 35(2):95–104.
31. Nankaku, M., Kanzaki, H., Tsuboyama, T., and Nakamura, T. (2005). Evaluation of hip fracture risk in relation to fall direction. *Osteoporos. Int.*, 16(11):1315–1320.
32. Pennycott, A., Wyss, D., Vallery, H., and Riener, R. (2011). Effects of added inertia and body weight support on lateral balance control during walking. *2011 IEEE Int. Conf. Rehabil. Robot.*, 2011:1–5.
33. Pijnappels, M., Kingma, I., Wezenberg, D., Reurink, G., and Van Dieën, J. H. (2010). Armed against falls: The contribution of arm movements to balance recovery after tripping. *Exp. Brain Res.*, 201(4):689–699.
34. Plooij, M., Keller, U., Sterke, B., Komi, S., Vallery, H., and von Zitzewitz, J. (2018). Design of RYSEN: An Intrinsically Safe and Low-Power Three-Dimensional Overground Body Weight Support. *IEEE Robot. Autom. Lett.*, 3(3):2253–2260.
35. Rousseeuw, P. J. and Hubert, M. (2011). Robust statistics for outlier detection. *Wiley Interdiscip. Rev. Data Min. Knowl. Discov.*, 1(1):73–79.
36. Tyson, S. F., Hanley, M., Chillala, J., Selley, A., and Tallis, R. C. (2006). Balance disability after stroke. *Phys. Ther.*, 86(1):30–38.
37. Vallery, H., Lutz, P., Von Zitzewitz, J., Rauter, G., Fritschi, M., Everarts, C., Ronsse, R., Curt, A., and Bolliger, M. (2013). Multidirectional transparent support for overground gait training. *IEEE Int. Conf. Rehabil. Robot.*
38. Van Thuc, T. and Yamamoto, S.-i. (2017). Investigation of the "pendulum effect" during gait locomotion under the novel body weight support system and counter weight system. In *International Conference for Innovation in Biomedical Engineering and Life Sciences*, pages 89–93. Springer.
39. Whittle, M. W. (1997). Three-dimensional motion of the center of gravity of the body during walking. *Hum. Mov. Sci.*, 16(2-3):347–355.
40. Winter, D. A. (2009). *Biomechanics and motor control of human movement*. John Wiley & Sons.
41. Wu, M., Brown, G., and Gordon, K. E. (2017). Control of locomotor stability in stabilizing and destabilizing environments. *Gait Posture*, 55(April):191–198.
42. Wu, M. M., Brown, G. L., Woodward, J. L., Bruijn, S. M., and Gordon, K. E. (2020). A novel Movement Amplification environment reveals effects of controlling lateral centre of mass motion on gait stability and metabolic cost.
43. Zeni, J. A., Richards, J. G., and Higginson, J. S. (2008). Two simple methods for determining gait events during treadmill and overground walking using kinematic data. *Gait Posture*, 27(4):710–714.

A: Informed Consent, Experiment Checklist, and Debriefing Forms

Informed Consent Form

Research Study:
Influence of body weight unloading on lateral balance strategies

Delft University of Technology

Informed Consent Form

This informed consent form is for individuals who are invited to participate in this TU Delft study about the effects of partial body-weight support on the lateral balance strategies during walking.

Researchers:	Nathan Fopma (contact), Andrew Berry, Saher Jabeen, Daniel Lemus, Patricia Baines, Romain Valette
Supervisor:	Heike Vallery
Organization Name:	Delft Technical University (TU Delft)
Faculty:	Biomechanical Engineering Department, Mechanical, Materials and Maritime Engineering (3ME) Faculty, TU Delft

Below is a brief introduction to the study and your role in it. If you agree to participate after reading this information, please sign the certificate of consent at the end of this form. You will receive a full copy of your signed Informed Consent Form, upon request.

Information Sheet

Introduction:
During walking a human has to actively control their lateral balance in order to stay upright and not fall sideways. Body weight unloading is commonly used to train individuals with gait impairments whom lack the muscle strength to support their own body weight. This research aims to investigate the effect of body weight unloading on lateral balancing by healthy humans. The results of this study will help to understand the interplay between the lateral balancing strategies and helps to identify possible effects the body weight unloading may have on training impaired gait. The research will also aid further development of the used body weight unloading device (RYSEN – Motek Medical B.V.).

Qualification:
You are a healthy adult (18 years or older) who weighs between 50 to 90 kg. To the best of your knowledge, you do not suffer from health issues which affect your movement in daily life activities. To participate, you must be in Delft on the experiment days.

Your role and time commitment:
Before starting the experiment, you are weighed in order to initialize the experimental setup according to your weight. After recording your weight, you are asked to wear a full body harness. A full-body reflective-marker set will then be placed on your body to facilitate the motion capture system. After this, a calibration procedure for the measurement set-up is performed, in which you will be asked to stand in the measurement space and mimic the movements of the experimenter. After the calibration procedure, you will be asked to walk multiple passes over a walkway to record measurements of unsupported gait. The full body harness is then supported from the RYSEN device and some time will be spent in different unloading conditions to familiarize yourself with the device. After the familiarization, your walking will be recorded for 6 different conditions of the device. In each condition, you will have to walk over the walkway 20 times. This means a total of 7 trials (1 free-walking and 6 with RYSEN). The experiment is expected to take around 120 minutes.

Data acquisition:
Passive markers for 3D motion acquisition system will be attached to the area from your hip to your foot throughout the experiment. You are advised to wear tight-fitting clothes in order to maintain the accuracy of the motion tracking system. Additionally, you are advised to wear shorts so that the motion-capture markers can be placed directly on your skin. The markers can easily be removed afterwards. Additionally, the time taken for completing each trial and the number of steps taken while walking will be recorded. We can also provide the appropriate clothing at the lab.

Discomforts involved in participating:
Wearing a full body harness might make walking slightly discomforting initially but will not pose a problem once you are accustomed to it.

Data Policy:
Personal information such as your weight and height will be measured, and your age will be asked prior to the experiments. During the experiments, identifiable (full-body) video recordings will be made of your walking gait. All the recorded data will be anonymized and stored safely without access to external parties. Personal data, which links your anonymized data to yourself, will be stored separately and only the researchers may have access to it. The video recordings will not be kept for longer than 12 months. If any video recordings have to be stored for a longer time period or used for any type of publication (such as a presentation or open data article) this will only happen with your consent. Any other identifiable data (such as name, email address, telephone number) are stored separately from the recorded data and will not be kept for longer than 6 months. All information will be archived so that no one except the researchers and supervisors as listed above will have access to the data. On request, you will have access to your own data. You may discuss with other participants after the study period, but please respect the confidentiality of others' participation in the study. All data is made anonymous for publication purposes. The anonymized data will be processed and uploaded to an online repository in the advent of a possible publication.

Participant's rights:
Participation in this research study is completely voluntary. Even after you agree to participate and begin the study, you are still free to withdraw at any time and for any reason. You have the right to ask that any data you have supplied to that point be withdrawn/destroyed, without penalty. You have the right to omit or refuse to answer or respond to any question that is asked, without penalty. You have the right to have your questions about the procedures answered (unless answering these questions would interfere with the study's outcome). If any questions arise as a result of reading this information sheet, you need to ask the investigators before the start of the experiment.

Cost, reimbursement and compensation:
No cost, reimbursement or compensation are applicable for this study.

For further information:
The investigators and supervisors listed above will gladly answer your questions about this study at any time. If you are interested in the final results of this study, you can contact one of the investigators or supervisors. For questions, please contact:
Nathan Fopma at n.c.fopma@student.tudelft.nl, +31639032486.

Informed Consent Form

Please tick the appropriate boxes

	Study Participation and recorded data	YES	NO
1	I consent voluntarily to be a participant in this study. I understand that I can refuse to answer questions and that I can withdraw from the study at any time, without giving any reason.	☐	☐
2	I understand that taking part in the study involves video recordings being made that are identifiable. I agree that those video recordings are made during the experiments.	☐	☐
3	I understand that during the experiments, sensor data is recorded by motion capture equipment, force plates, electromyographic sensors, and by the RYSEN device itself.	☐	☐
4	I understand that I will be asked questions regarding my age and that my height and weight will be measured.	☐	☐
	Data Use		
5	I understand that information I provide will be used for the master thesis and a possible research article of Nathan Fopma.	☐	☐
6	I understand that personal information that can identify me (such as my name, email address, and telephone number) will not be shared beyond the research team.	☐	☐
7	I understand that personal information and recorded data will be stored separately.	☐	☐
8	I understand that any identifiable data (such as the video recordings) will be either removed or anonymized a maximum of 12 months after the experiments.	☐	☐
9	I agree that the recorded data in the experiments can be used (anonymized) in research outputs and can be published as open data.	☐	☐
10	I consent that non-anonymized photos or videos taken in this experiment can be shown in public presentations	☐	☐
11	I understand that I may request my data at any time, and that I can make corrections to any inaccurate data that I provided. I also understand that I have to 'right to be forgotten' and can request the deletion of my data.	☐	☐

Consent Certificate

I have read and understand the information above and have had the opportunity to ask questions and my questions have been answered satisfactorily. By signing this form, I voluntarily consent to participate as a research participant in this study.

_____

Name of Participant (BLOCK CAPITALS)

_____ _____

Signature of Participant Date

_____

Name of Researcher (BLOCK CAPITALS)

_____ _____

Signature of Researcher Date

If you would like a copy of this consent form to keep, please ask the researcher.

Checklist

Delft University of Technology

Checklist

Participant-#	
Date	
Time	

Pre-Experiment

1. Study information sheet and informed consent signed?
2. Participant mass in kg
3. Participant height in m
4. Participant age in years
5. Note participant name linked to participant number in identifier database

Marker placement

6. RYSEN-Harness outfitted
7. Place dynamic markers
8. Take photos (front and back)

AIM Model Calibration

9. Static calibration (*P#-static*) recorded (10 seconds)
10. Dynamic calibration (*P#-dynamic*) recorded (60 seconds)

Baseline

11. Calibrate foot placement and place tape (check until 3 successful passes)
12. Record 10 back-and-forth passes (*P#-baseline*)

Familiarization

13. Let the participant walk in each of the experimental conditions
14. Perform foot placement calibration for each condition, place tapes

Experiments

15. Condition order

16. Record conditions (*P#-BWS%-<H_PP/D>)*

Debriefing

17. Detach markers
18. Debriefing sheet

Condition	UpwardForce	PivotPoint
1	20%	Transparent
2	40%	Transparent
3	60%	Transparent
4	40%	5 m
5	40%	2 m
6	40%	Damping

Order of conditions (Balanced Latin Square)
http://www.stat.purdue.edu/research/technical_reports/pdfs/1980/tr80-26.pdf

P#	C1	C2	C3	C4	C5	C6
1	1	2	3	4	5	6
2	2	4	1	6	3	5
3	5	3	6	1	4	2
4	4	6	2	5	1	3
5	6	5	4	3	2	1
6	3	1	5	2	6	4
7	1	2	3	4	5	6
8	2	4	1	6	3	5
9	5	3	6	1	4	2
10	4	6	2	5	1	3
11	6	5	4	3	2	1
12	3	1	5	2	6	4
13	1	2	3	4	5	6
14	2	4	1	6	3	5
15	5	3	6	1	4	2
16	4	6	2	5	1	3
17	6	5	4	3	2	1
18	3	1	5	2	6	4

Debriefing Sheet

Research Study:
Influence of body weight unloading on lateral balance strategies

Delft University of Technology

Debriefing Sheet

This debriefing sheet is for individuals who participated in the study investigating the effects of partial body-weight support on the lateral balance strategies during walking.

Researchers:	Nathan Fopma (contact), Andrew Berry, Saher Jabeen, Romain Valette
Supervisor:	Prof. Heike Vallery
Organization Name:	Delft Technical University (TU Delft)
Faculty:	Biomechanical Engineering Department, Mechanical, Materials and Maritime Engineering (3ME) Faculty, TU Delft

During walking you have to actively control your lateral motion in order to remain upright and not fall sideways – you control your body dynamics in order to remain laterally balanced. This is done by controlling the external forces on the body, which during regular walking is the ground reaction force under the feet. The magnitude, direction and position of the Ground Reaction Force (GRF) is determined by several balancing strategies. Body weight support puts other external forces on the body and therefore changes the dynamics of lateral balancing.

The most efficient way of maintaining lateral balance is the *foot placement strategy*. However, it seems that the vertical body weight unloading force has a large influence on the dynamics of the foot placement strategy. Therefore, in this research it is hypothesized that the body weight unloading force decreases the effectiveness of the foot placement strategy, which consequently increases the reliance on alternative balancing strategies. These alternative balancing strategies include creating a torque around the ankle joint with the ankle muscles, using the inertia of the body (e.g. laterally moving the trunk or swinging the arms) and regulating the push-off force by using the calf muscles.

Most body weight support devices work with systems that utilize a rail to move the weight support along a straight line. A side-effect of these systems is that a lateral movement with respect to this rail causes a lateral force towards this line. The RYSEN device used in the experiments is able to track forces laterally, which largely reduces these lateral forces. It is also possible to produce artificially induced lateral forces. In the experiments, the 'straight-line' body weight support dynamics was virtually implemented in order to make a direct comparison between the system dynamics.

Thank you again for your participation!

B: Walkway and force plates

Fig. A1 shows the steps made by the participants across the walkway. The four black footsteps represent the steps that were used to extract the outcome measures. Fig. A2 shows the mean step length and step width across all the conditions for each stepping location. Step 1 and step 2 had contact with the force plates, step 3 and 4 only made contact with the walkway that followed the two force plates.

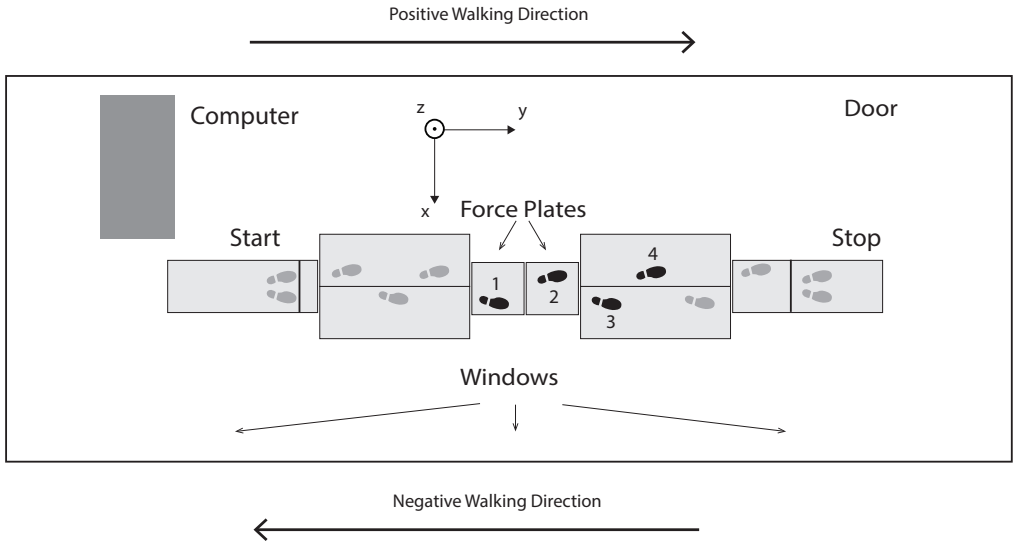

Fig. A1. The walkway used in the experiment from a top view. The footsteps in black represent the steps used for analysis of the data. Step 1 and 2 are on the force plates, step 3 and 4 on the walkway behind the force plate.

Friedman's ANOVA and Bonferonni corrected Wilcoxon Signed-Rank tests show that there are significant differences between the stepping locations for the step length and step width. This could indicate that steady-state walking was not reached due to the short walkway length. Another interpretation could be that the forceplates influenced the stepping location. The participants were instructed to keep their gaze at eye level. Regardless of the instruction, some participants were caught quickly glancing at the forceplates right before stepping on them.

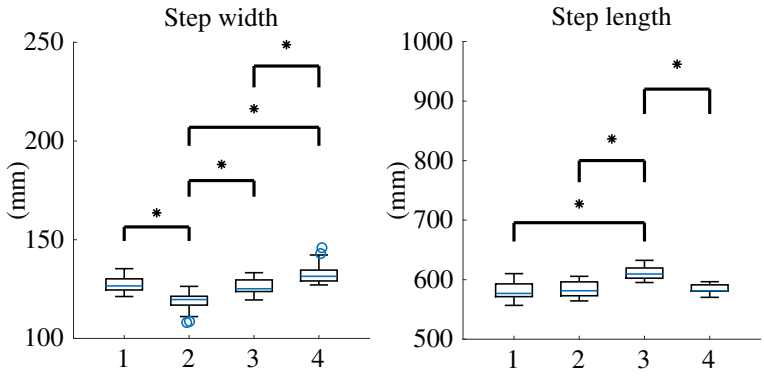

Fig. A2. Mean across all conditions step length and step width values for the 4 stepping locations on the walkway.

C: Marker placement

A lower-extremity marker set was used for this experiment.

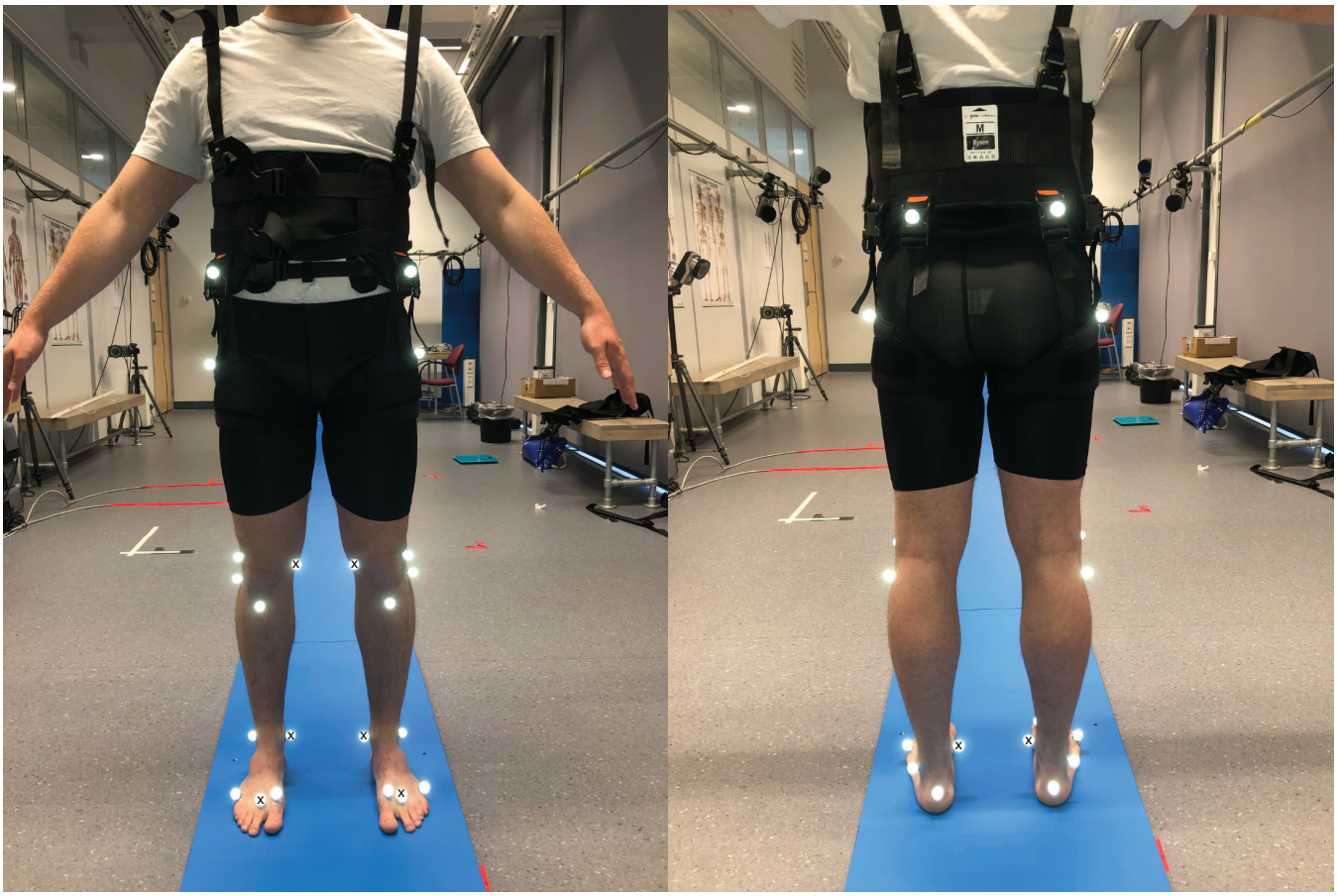

Fig. A3. Placement of the motion capture markers on the lower extremity. A black cross through the marker indicates that this marker was only used for performing a static calibration.

D: Ankle joint and foot progression

Fig. A4 shows the ankle joint position used to compute the step width in this experiment. We chose to compute the step width based on the mediolateral distance between the ankle joints because this would be least biased by the foot progression angle and shifting of the CoP by the ankle strategy. All of the vectors shown in the image are two-dimensional, they represent vectors with x and z coordinates. First, a vector is computed that describes the direction of the midline of the foot in the global frame as follows:

$$\boldsymbol{r}_{\text{mid}} = (\boldsymbol{r}_{\text{FM1}} + \boldsymbol{r}_{\text{FM5}})/2 - \boldsymbol{r}_{\text{FCC}}, \tag{16}$$

which is normalized as

$$\boldsymbol{u}_{\text{mid}} = \frac{\boldsymbol{r}_{\text{mid}}}{||\boldsymbol{r}_{\text{mid}}||}. \tag{17}$$

Then, the vector $\boldsymbol{r}_{\text{FAL}} - \boldsymbol{r}_{\text{FCC}}$ is projected on the midline of the foot and multiplied with $\boldsymbol{u}_{\text{mid}}$. By adding this vector to $\boldsymbol{r}_{\text{FCC}}$, the position of the ankle joint is finally computed as

$$\boldsymbol{r}_{\text{ankle}} = \big((\boldsymbol{r}_{\text{FAL}} - \boldsymbol{r}_{\text{FCC}}) \cdot \boldsymbol{u}_{\text{mid}}\big) \cdot \boldsymbol{u}_{\text{mid}} + \boldsymbol{r}_{\text{FCC}} \tag{18}$$

The step width is then computed by subtracting the x-coordinate from the right $\boldsymbol{r}_{\text{ankle}}$ from the left $\boldsymbol{r}_{\text{ankle}}$ in the middle of the double support phase. The foot progression angle is computed by finding the angular displacement between global z-axis and $\boldsymbol{u}_{\text{mid}}$ as

$$\text{Foot Progression} = \arctan \frac{u_{\text{mid,x}}}{u_{\text{mid,z}}} \tag{19}$$

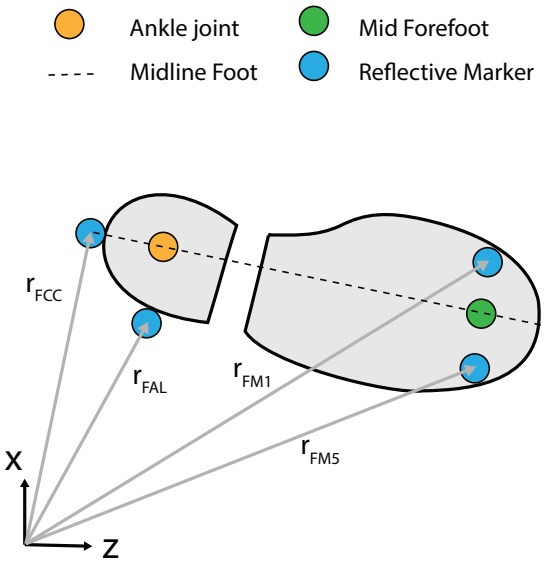

Fig. A4. Top view of the foot, motion capture markers, ankle joint and midline of the foot.

E: Relative contribution of balance strategies

In the methods section of this article, the modeled contribution of the CoP-displacement mechanism and counter-rotation strategy to the $F_{\text{GRF}x}$ was derived. This eventually led to the following equation:

$$\underbrace{F_{\text{GRF}x}}_{F_{\text{GRF}x:\text{Total}}} = \underbrace{\frac{x_{\text{CoP}} - x_{\text{CoM}}}{l_{\text{eq}}} F_{\text{GRF}y}}_{F_{\text{GRF}x:\text{CoP}}} + \underbrace{\frac{T_{\text{i}}}{l_{\text{eq}}}}_{F_{\text{GRF}x:\text{CR}}} . \tag{20}$$

To determine the relative contribution of the CoP-displacement mechanism to the $F_{\text{GRF}x}$, the coefficient of determination R^2 was computed.

$$R^2 = 1 - \frac{\text{var}\left(\boldsymbol{F}_{\text{GRF:CoP}} - \boldsymbol{F}_{\text{GRF}x:\text{Total}}\right)}{\text{var}\left(\boldsymbol{F}_{\text{GRF}x:\text{Total}}\right)}. \tag{21}$$

Fig. A5 shows a density scatter plot of the total $F_{\text{GRF}x}$ and the modeled $F_{\text{GRF}x}$ that can be attributed to the CoP-displacement mechanism for one participant. Fig. A6 shows the same plot, but then with all the data of all of the participants combined. Even though each of the plots show a scatter around the unity line, the 40G and 60G conditions clearly show a broader scatter with respect to the total range.

For some further illustration, Fig. A7 and Fig. A8 show the trajectory of $F_{\text{GRF}x:\text{Total}}$ and $F_{\text{GRF}x:\text{CoP}}$ for one walkway pass in respectively the RW and 60G conditions. Clearly, in these examples, there is a larger residual in the 60G condition.

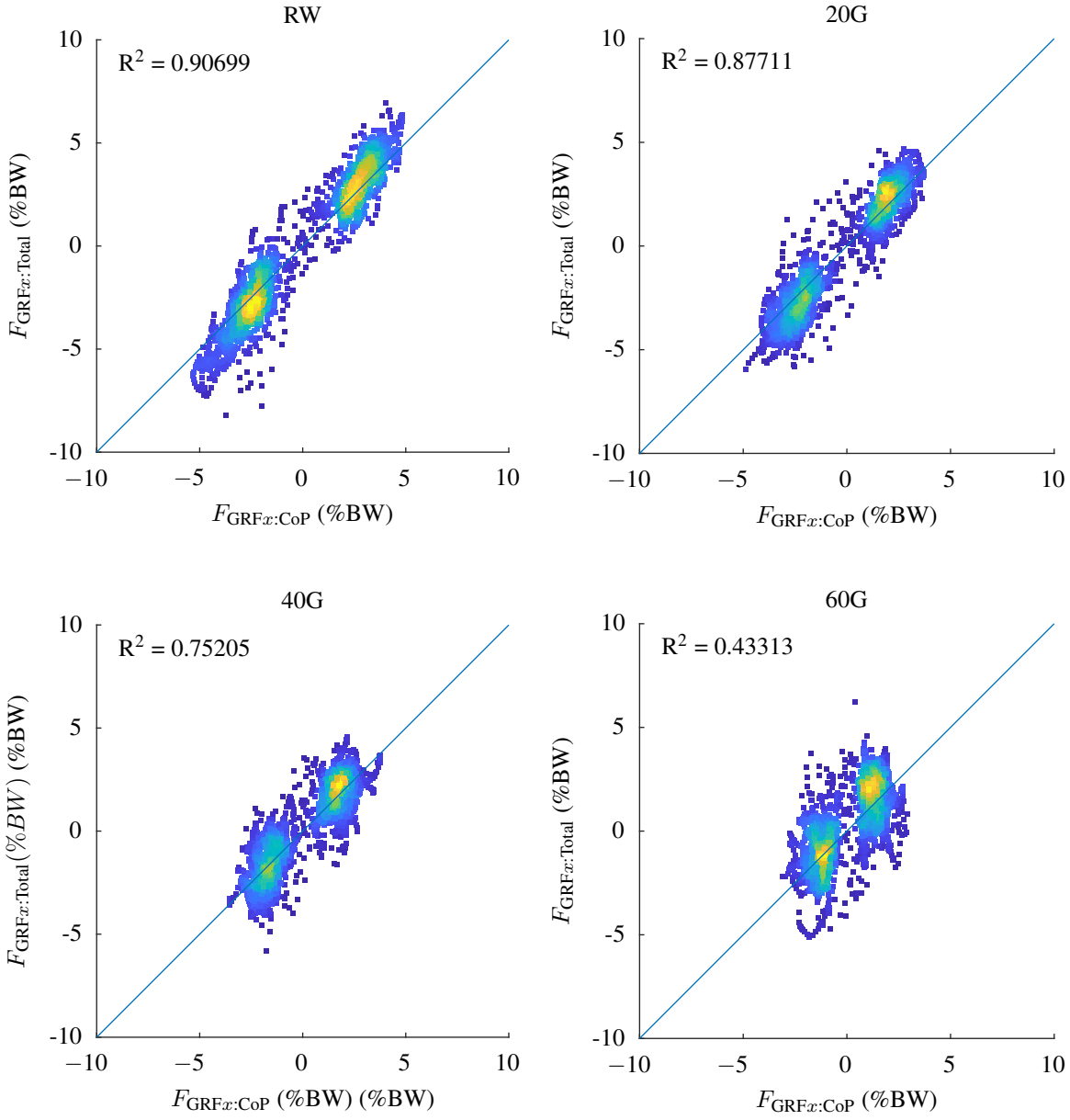

Fig. A5. Density scatter plot of the $F_{\text{GRF}x\text{:CoP}}$ versus the $F_{\text{GRF}x\text{:Total}}$ for all walkway passes in each vertical unloading condition of participant P12. The straight line in the plot represents the unity line ($F_{\text{GRF}x\text{:Total}} = F_{\text{GRF}x\text{:CoP}}$).

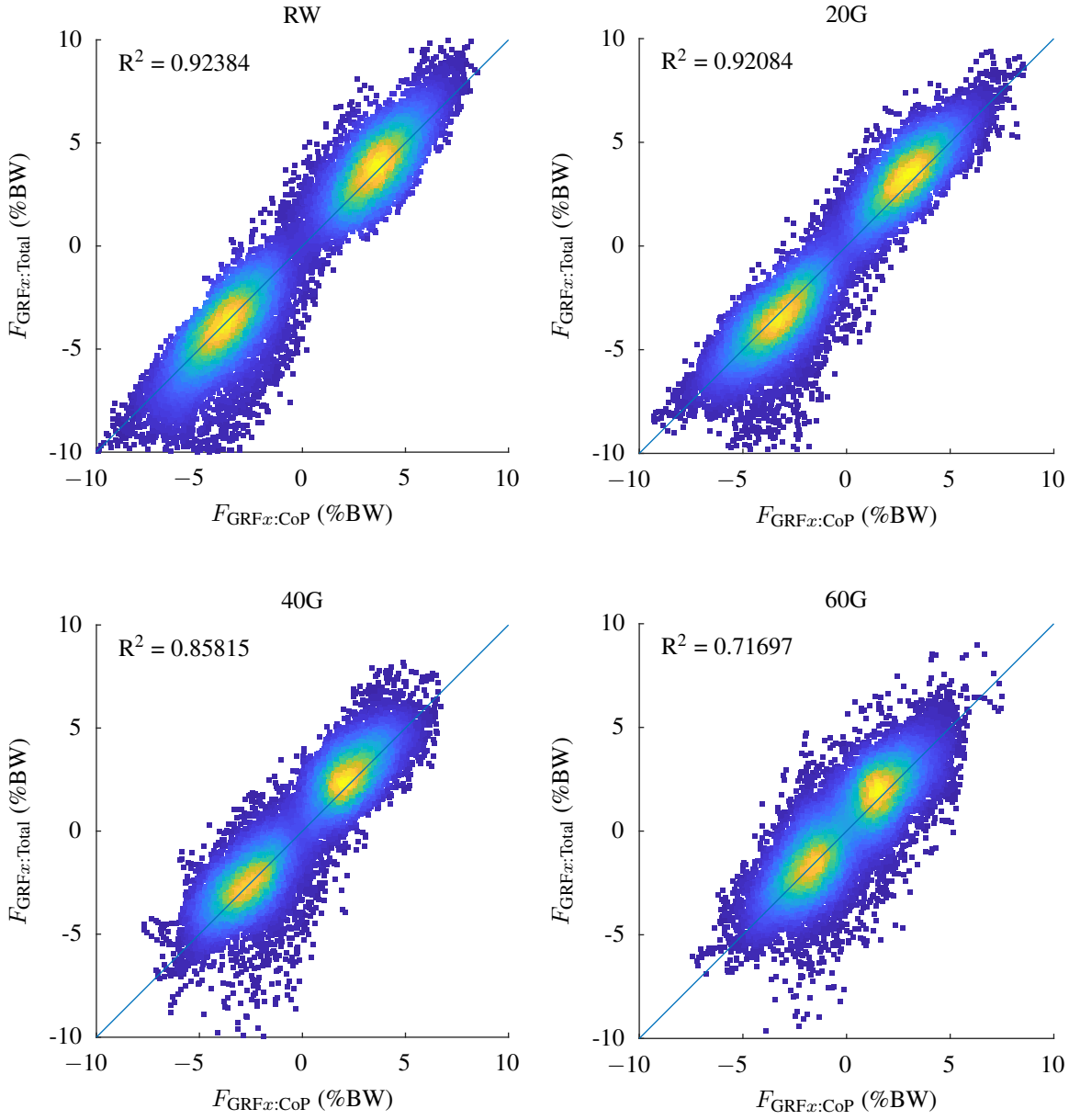

Fig. A6. Density scatter plot of the $F_{\text{GRF}x\text{:CoP}}$ versus the $F_{\text{GRF}x\text{:Total}}$ for all walkway passes in each vertical unloading condition of all participants. The straight line in the plot represents the unity line ($F_{\text{GRF}x\text{:Total}} = F_{\text{GRF}x\text{:CoP}}$).

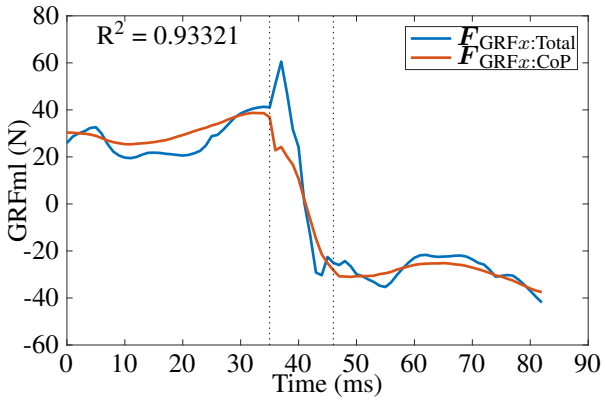

Fig. A7. The trajectory across one walkway pass by one participant in the RW condition of $F_{GRFx:Total}$ and $F_{GRFx:CoP}$.

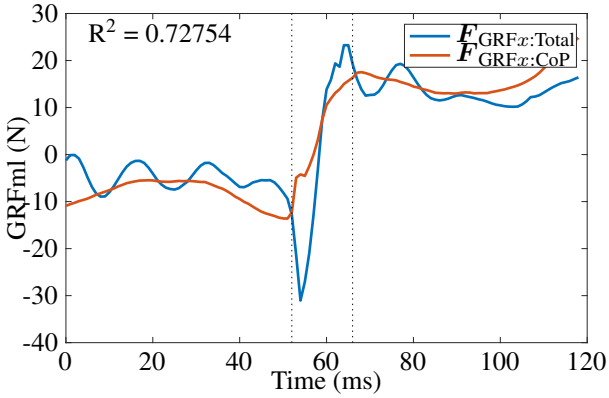

Fig. A8. The trajectory across one walkway pass by one participant in the 60G condition of $F_{GRFx:Total}$ and $F_{GRFx:CoP}$.

F: Removing between subject variance

The between-subject variance has been removed by transforming the data so that the participant mean is equal to the grand mean for each participant (Loftus and Masson (1994)). To do this, from a participant their outcome measures an adjustment factor is subtracted. This adjustment factor is the difference between the participant mean (mean of outcome measure across all conditions for a single participant) and the grand mean (mean of outcome measures across all conditions for all the participants). Table A1 shows the untransformed step width data. To transform the data of P1, $135 - 127 = 8$ is subtracted from each of the scores. To transform the data of P2, $117 - 127 = -10$ is subtracted from each of the scores. Table A2 shows the transformed data. The transformation does not affect the within-subject differences and therefore has no effect on the repeated-measures statistical tests done on the data. The visualisation by the boxplots better represents the actual effect of the conditions on the outcome measures.

Table A1. Raw step width data in the different unloading conditions

Participant	RW	20G	40G	60G	Participant Mean
P1	123	141	127	150	135
P2	110	118	120	121	117
P3	122	118	129	123	123
P4	99	103	104	109	104
P5	133	137	133	139	136
P6	130	132	148	156	141
P7	145	172	141	183	160
P8	108	111	121	121	115
P9	84	77	79	70	77
P10	137	142	131	123	133
P11	85	84	87	92	87
P12	134	142	144	150	143
P13	164	167	158	190	170
P14	140	133	135	165	143
P15	111	105	131	126	118
Condition Mean	122	125	126	134	**Grand Mean** 127

Table A2. Transformed step width data in the different unloading conditions

Participant	RW	20G	40G	60G	Participant Mean
P1	115	133	119	141	127
P2	120	127	130	130	127
P3	126	121	133	127	127
P4	122	126	127	132	127
P5	125	129	124	130	127
P6	115	117	133	141	127
P7	111	138	108	150	127
P8	120	122	133	133	127
P9	133	126	128	120	127
P10	131	136	125	116	127
P11	125	124	127	132	127
P12	119	126	129	135	127
P13	121	124	115	147	127
P14	124	116	119	148	127
P15	120	113	140	134	127
Condition Mean	122	125	126	134	**Grand Mean** 127

Fig. A9 shows the boxplots for the step width data where the between-subject variance is still present and the step width data where the between-subject variance has been removed. The strength of this transformation becomes even more apparent when we plot a outcome measure that has an obvious within-subject effect, but a lot of between-subject variance. To illustrate that, Fig. A10 shows boxplots for the foot progression in this experiment.

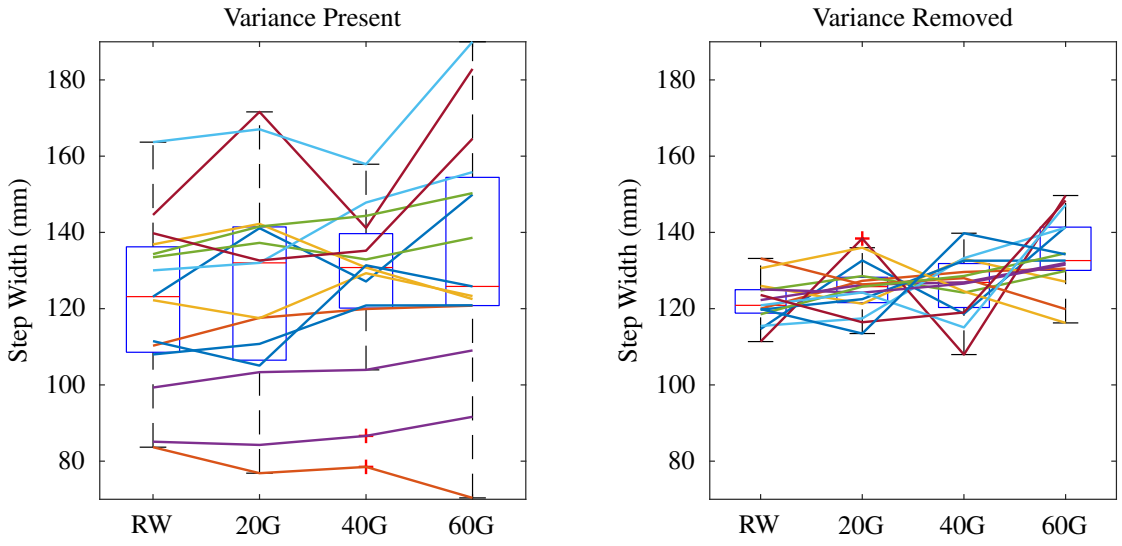

Fig. A9. Removing the between subject variance from the step width data.

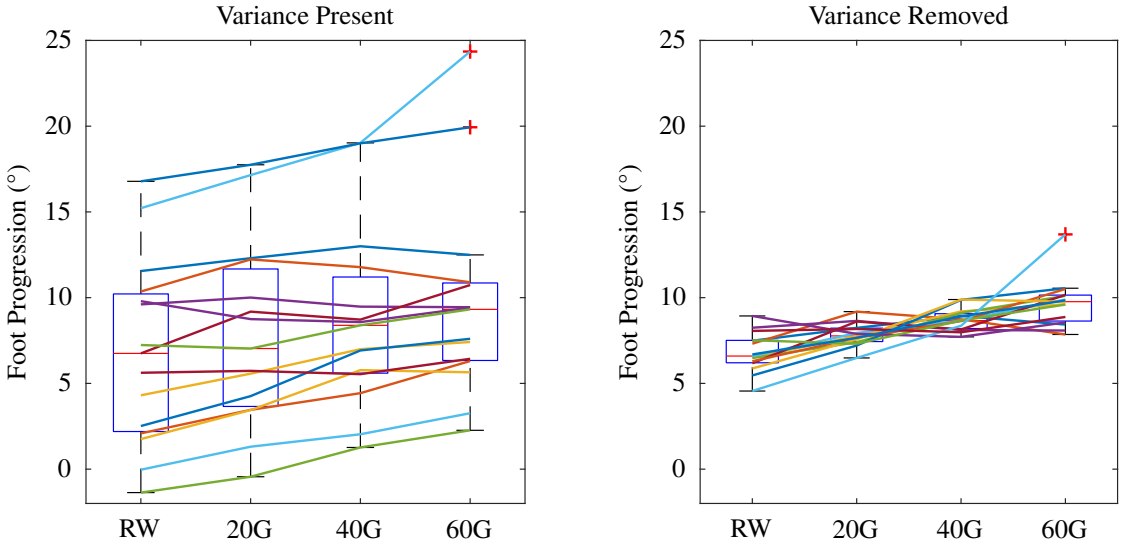

Fig. A10. Removing the between subject variance from the foot progression data.

G: Statistical analysis

Parametric tests (such as the repeated-measures ANOVA and dependent t-tests) are preferred when testing a hypothesis because they have a higher power of detecting an effect if there is one. However, they rely on the assumption that the data is normally distributed and does not contain any outliers.

To test whether the data contained outliers, the between-subject variance was first removed from the data by subtracting the difference between the participant mean and the grand mean from each data point. This data was first assessed within each condition on outliers by using z-scores based on the median and the median of all absolute deviations (35). A moderate- and extreme outlier were defined as a point outside of respectively the [3.33% 96.67%] and [1% 99%] interval of the z-scores. If more than one moderate outlier (probability of 6.67% per condition with 15 participants) or any extreme outlier were identified, the non-parametric tests were used for that outcome measure. If there was an acceptable number of outliers, the normality of the residual was assessed by checking the kurtosis and skewness of the distributions and using the Shapiro-Wilks and Kolgomorov-Smirnov tests.

An overview of the outcomes of the statistical tests are provided in Table A3 and Table A4.

Table A3. Test statistics for the effect of vertical unloading. Wilcoxon Signed-Rank tests were performed against the baseline of regular walking. Bold numbers reflect test statistics that correspond to a significant finding ($\alpha < 0.16667$).

	Friedman		Wilcoxon Signed-Rank									
			RW	20G			40G			60G		
Outcome Measure	$\chi^2(3)$	p	Mdn	Mdn Δ	p	r	Mdn Δ	p	r	Mdn Δ	p	r
Step Width (mm)	**13.2**	**0.004**	123	9	0.211	0.32	8	0.125	0.40	**3**	**0.012**	**0.65**
Step Width Var (mm)	5.2	0.155	21	1	0.191	0.34	-1	0.532	-0.16	2	0.031	0.56
R^2 (-)	**35.6**	**0.000**	0.92	-0.01	0.334	-0.25	**-0.05**	**0.003**	**-0.76**	**-0.18**	**0.001**	**-0.88**
CoP Shift (mm)	4.0	0.266	6	1	0.256	0.29	2	0.776	-0.07	0	0.256	0.29
CoM Displacement (mm)	**21.5**	**0.000**	40	0	0.650	-0.12	**-10**	**0.003**	**-0.76**	**-14**	**0.005**	**-0.73**
CoM Velocity (mm/s)	**27.7**	**0.000**	118	-4	0.211	-0.32	**-33**	**0.001**	**-0.87**	**-50**	**0.001**	**-0.85**
Margin of Stability (mm)	**18.3**	**0.000**	32	-2	0.427	0.21	**8**	**0.002**	**0.81**	**16**	**0.003**	**0.78**
Foot Progression (°)	**18.8**	**0.000**	6.7	**0.3**	**0.004**	**0.75**	**1.6**	**0.003**	**0.78**	**2.6**	**0.001**	**0.84**
Double Support (stride%)	**43.9**	**0.000**	26.2	**-1.2**	**0.001**	**-0.82**	**-4.3**	**0.001**	**-0.88**	**-7.5**	**0.001**	**-0.88**
Step Length (mm)	**24.4**	**0.000**	611	**-25**	**0.005**	**-0.73**	**-22**	**0.005**	**-0.73**	**-49**	**0.001**	**-0.82**
Step Length Var (mm)	**18.3**	**0.000**	24	4	0.865	0.04	5	0.460	0.19	**10**	**0.003**	**0.78**
Walking Speed (m/s)	**14.5**	**0.002**	1.17	-0.02	0.100	-0.43	-0.03	0.256	-0.29	**-0.13**	**0.006**	**-0.70**
Cadence (steps/s)	**16.4**	**0.001**	1.8	0.0	0.691	-0.10	0.0	0.570	-0.15	**-0.1**	**0.005**	**-0.72**
Com-CoP Distance (mm)	**33.2**	**0.000**	50	1	0.047	0.51	**7**	**0.001**	**0.88**	**13**	**0.001**	**0.88**
Base of Support (mm)	**15.2**	**0.002**	141	9	0.112	0.41	**15**	**0.006**	**0.70**	**25**	**0.005**	**0.72**
XCoM Displacement (mm)	8.2	0.042	83	5	0.191	0.34	-9	0.088	-0.44	-14	0.363	-0.23
CoP variability (mm)	10.0	0.019	5.136	0.556	0.156	0.37	0.197	0.955	0.01	1.896	0.041	0.53
r_c	**35.7**	**0.000**	0.94	0.00	0.125	-0.40	**-0.04**	**0.003**	**-0.76**	**-0.11**	**0.001**	**-0.88**

Table A4. Test statistics for the effect of lateral support. Wilcoxon Signed-Rank tests were performed against the baseline of 40% unloading with lateral guiding. Bold numbers reflect test statistics that correspond to a significant finding ($\alpha < 0.16667$).

	Friedman		Wilcoxon Signed-Rank									
			40G	K_L			K_H			D		
Outcome Measure	$\chi^2(3)$	p	Mdn	Mdn Δ	p	r	Mdn Δ	p	r	Mdn Δ	p	r
Step Width (mm)	0.0	0.998	131	0	0.570	-0.15	5	0.820	-0.06	3	0.955	-0.01
Step Width Var (mm)	**11.4**	**0.010**	20	**-3**	**0.005**	**-0.73**	-2	0.156	-0.37	-2	0.061	-0.48
R^2 (-)	5.0	0.172	0.87	0.00	0.532	-0.16	0.00	0.334	-0.25	0.00	0.027	-0.57
CoP Shift (mm)	2.3	0.516	7	-2	0.334	0.25	-1	0.233	0.31	-1	0.427	0.21
CoM Displacement (mm)	4.0	0.257	30	-1	0.281	-0.28	1	0.733	-0.09	2	0.191	0.34
CoM Velocity (mm/s)	**8.0**	**0.045**	85	-4	0.650	-0.12	3	0.078	0.45	**10**	**0.006**	**0.70**
Margin of Stability (mm)	**10.1**	**0.018**	39	0	0.609	-0.13	-3	0.394	-0.22	-4	0.112	-0.41
Foot Progression (°)	2.0	0.564	8.4	-0.52	0.733	-0.09	-0.67	0.776	0.07	-0.02	0.910	-0.03
Double Support (stride%)	3.0	0.392	21.9	0.6	0.017	0.62	0.4	0.910	0.03	0.3	0.363	0.23
Step Length (mm)	2.4	0.486	589	-5	0.427	0.21	3	0.281	0.28	-3	0.307	0.26
Step Length Var (mm)	**8.4**	**0.039**	29	1	0.650	0.12	1	0.078	0.45	-1	0.910	0.03
Walking Speed (m/s)	1.8	0.615	1.14	0.04	0.570	0.15	0.03	0.394	0.22	0.03	0.173	0.35
Cadence (steps/s)	1.8	0.615	1.8	0.1	0.334	0.25	0.0	0.733	0.09	0.0	0.334	0.25
Com-CoP Distance (mm)	3.3	0.345	57	3	0.650	-0.12	-1	0.427	-0.21	2	0.363	-0.23
Base of Support (mm)	0.4	0.932	156	0	0.733	-0.09	-5	0.910	-0.03	-4	0.865	-0.04
XCoM Displacement (mm)	**6.8**	**0.080**	74	-2	0.532	-0.16	5	0.307	0.26	10	0.020	0.60
CoP variability (mm)	1.6	0.650	5	0	0.570	-0.15	1	0.427	0.21	1	0.460	0.19
r_c	3.2	0.356	0.903	0.008	0.532	0.16	-0.004	0.733	0.09	-0.015	0.233	-0.31

H: Relative difference to baseline

In this section, Fig. A11 and Fig. A12 show boxplots that visualize the relative difference of the outcome measures with respect to the baseline conditions (vertical unloading: RW, lateral support: 40G). The y-axis shows the relative difference with respect to the median of the baseline condition in percentages.

The percentual difference is calculated by subtracting the value of the outcome measure of the baseline condition (measure_b) from the outcome measure in a condition (measure_c), and dividing by the outcome measure of the baseline condition as follows:

$$\Delta\text{measure} = \frac{\text{measure}_\text{c} - \text{measure}_\text{b}}{\text{measure}_\text{b}} \cdot 100\%. \tag{22}$$

So, when a step width of 120 mm is measured in the 40G condition, and a step width of 100 mm in the RW condition, the percentual difference is equal to

$$\Delta\text{measure} = \frac{120 - 100}{100} \cdot 100\% = 20\%. \tag{23}$$

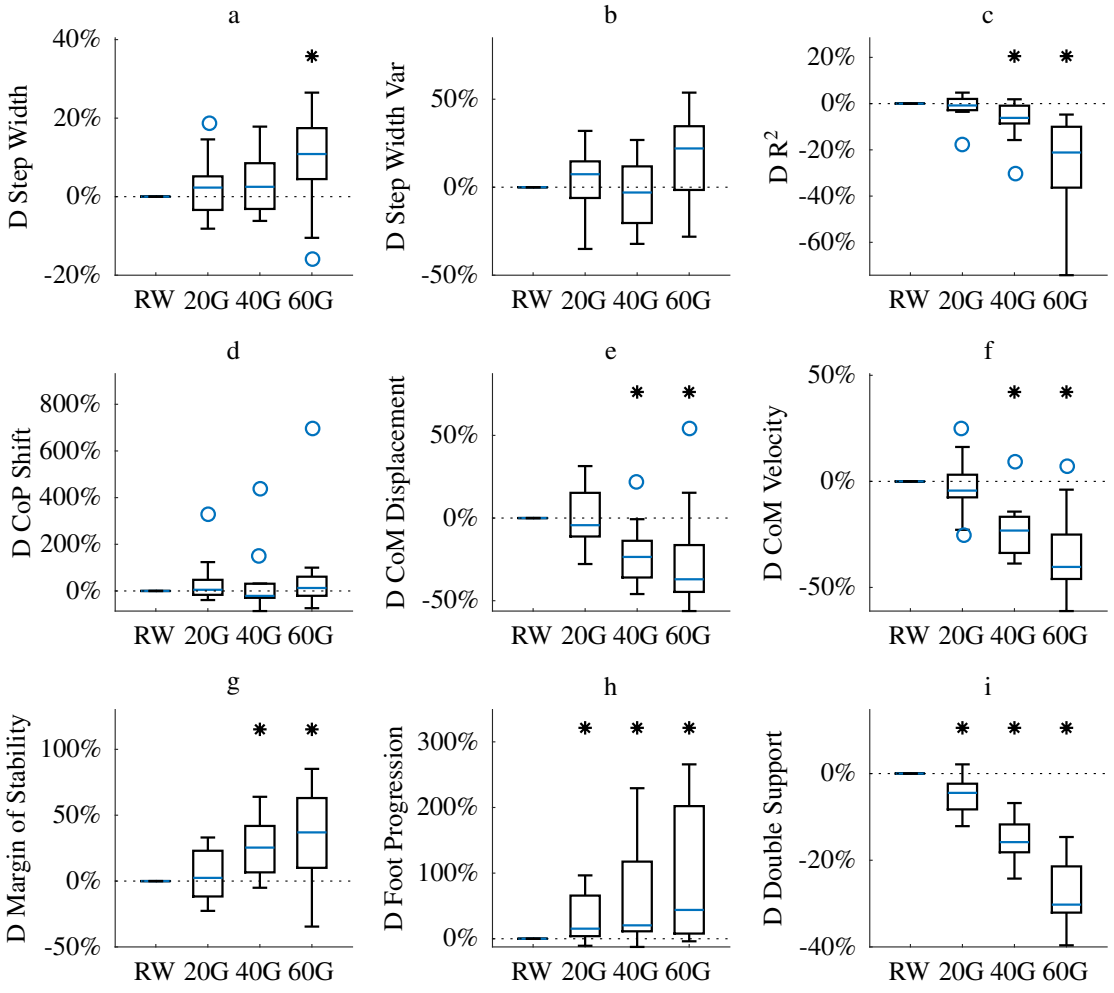

Fig. A11. Boxplots of the effect of vertical unloading on the outcome measures. The y-axis represents the relative difference to the 40G condition. An asterisk (*) above the boxplot indicates a significant difference to the RW condition.

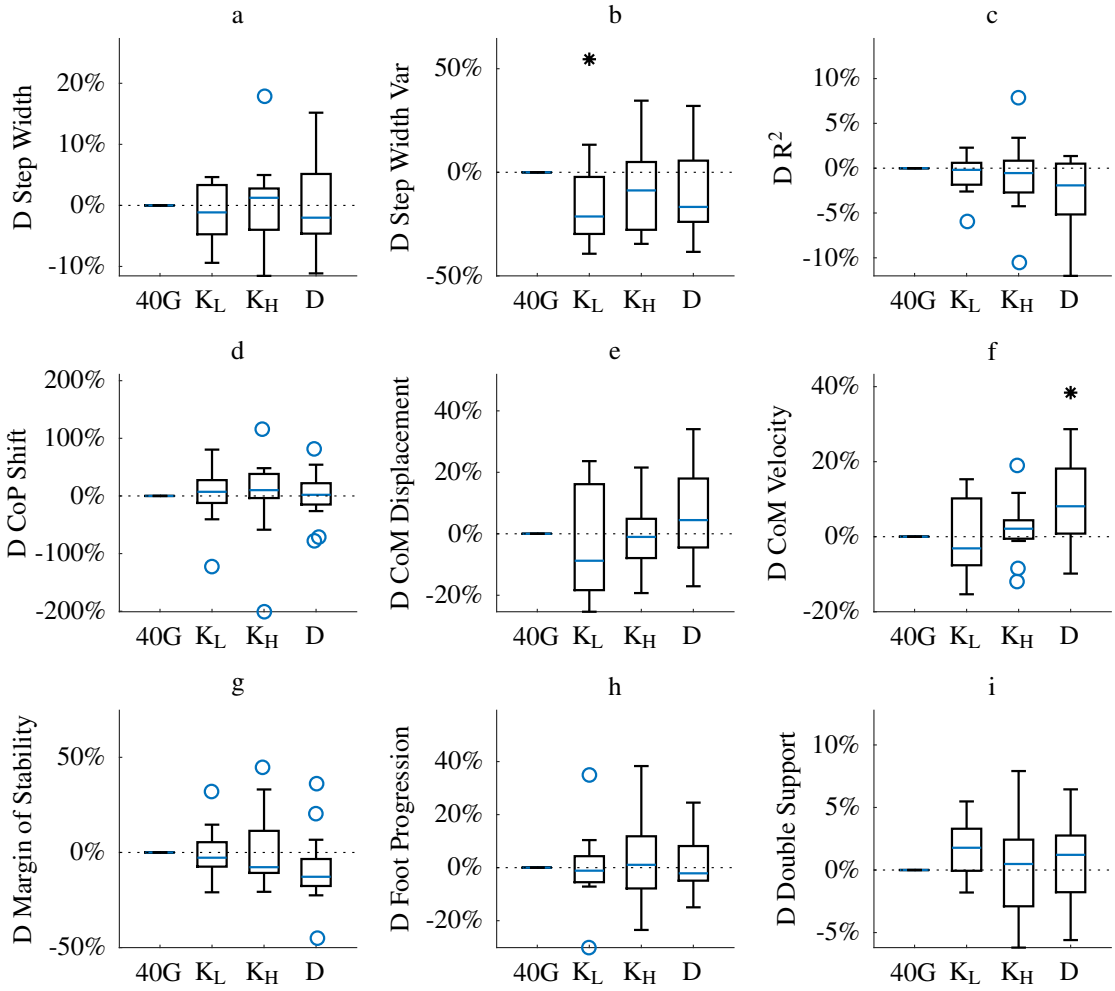

Fig. A12. Boxplots of the effect of lateral support on the outcome measures. The y-axis represents the relative difference to the 40G condition. An asterisk (*) above the boxplot indicates a significant difference to the 40G condition.

I: RYSEN lateral forces

Fig. A13 shows the RMS lateral force estimated by the RYSEN in the different conditions used in this experiment. The top plot shows that vertical unloading has an effect on the lateral support forces in the RYSEN. The bottom plot shows that the lateral support conditions did in fact have an effect on the lateral support forces.

Fig. A14 shows the normalized lateral force and normalized lateral displacement of the RYSEN to give a qualitative idea about their coupling. The bottom graph shows the behaviour when a stiffness of 0 is prescribed to the system and it behaves as in its LG mode. We see that in the LG mode, the force behaves similar to a damping. Each time when the slope of the displacement is at a peak, the damping is as well. When a stiffness is used as an input to the system, the displacement and force start to follow better.

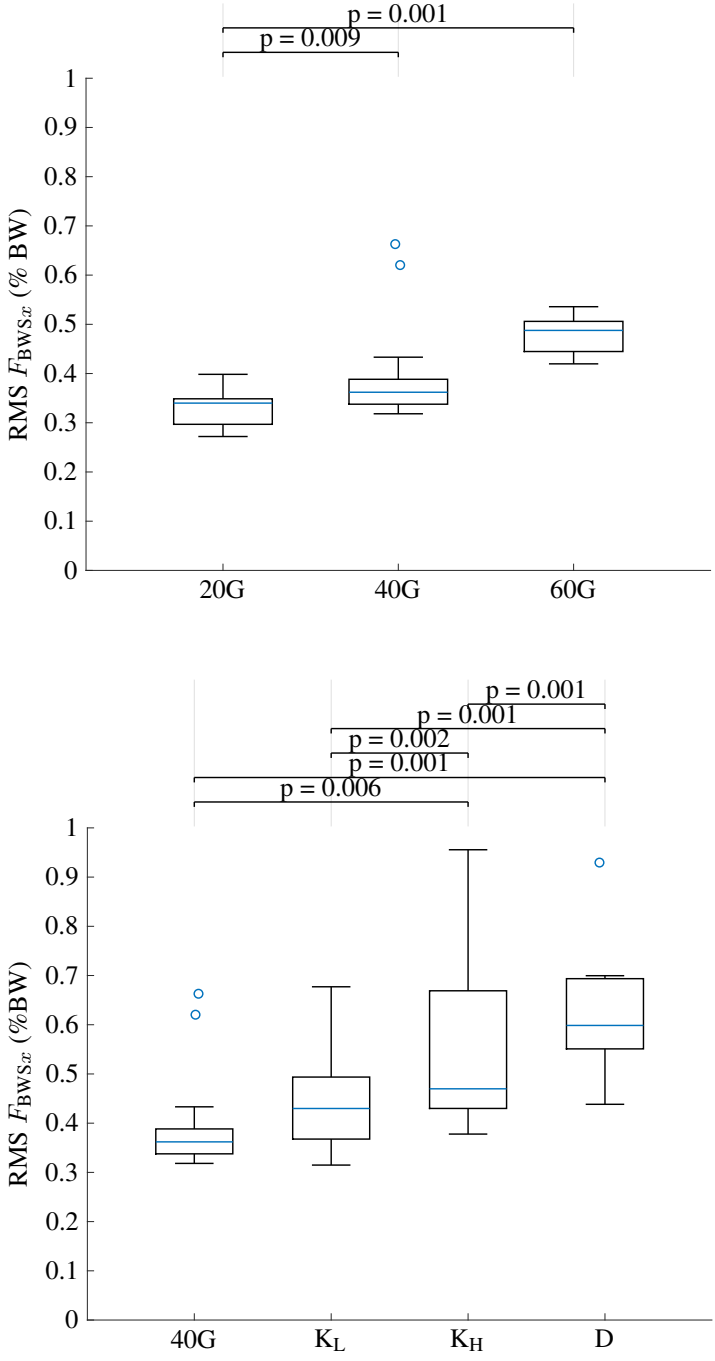

Fig. A13. RMS lateral forces estimated by the RYSEN in the different conditions.

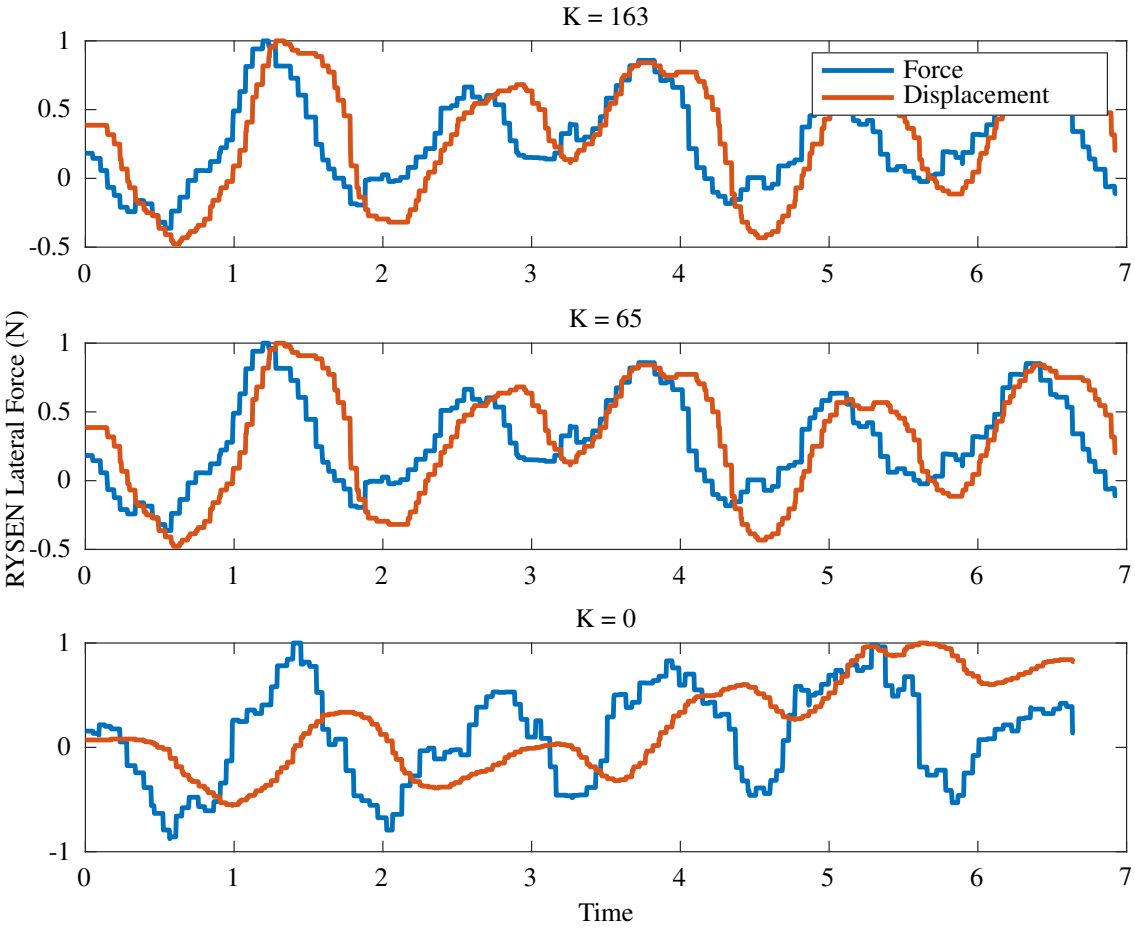

Fig. A14. Lateral displacement of the RYSEN and lateral forces plotted for three different stiffness conditions o fthe RYSEN.

J: Distance between CoM and CoP

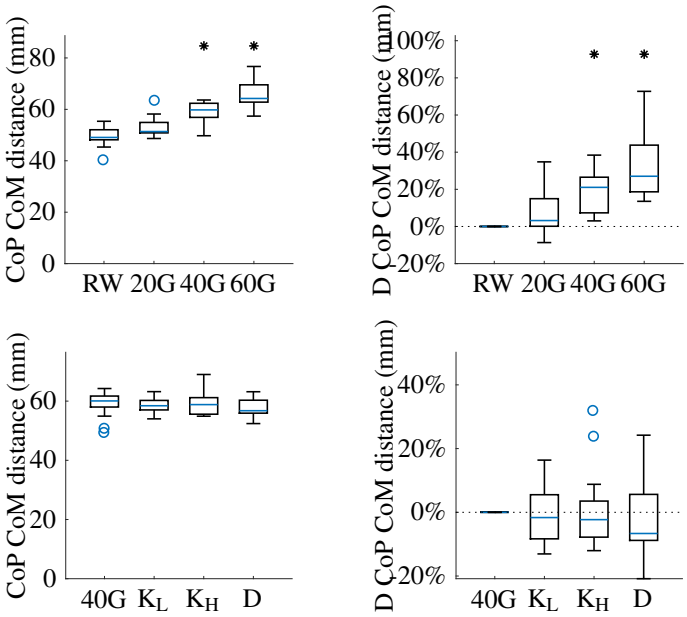

Fig. A15. The mean distance between the CoM and CoP during the single stance phase of walking. An asterisk (*) denotes a significant difference with respect to the first condition of the plot.

K: Ground Reaction Forces

This section illustrates some extra visualisations to interpret the effect of BWS on the ground reaction forces. The top two figures of **??** show the mean trajectories of $F_{\text{GRF}x}$ and $F_{\text{GRF}y}$. Their shapes are quite similar in the baseline condition, mostly due to the characteristic 'two-hump' shape that is present in both of the trajectories. However, as unloading increases, $F_{\text{GRF}y}$ keeps this characteristic shape, while $F_{\text{GRF}x}$ flattens. When the impulse across the single stance phase is computed, it becomes apparent that both the mediolateral and vertical impulse decrease significantly when unloading increases. To further analyze the interplay between these two forces, the ratio between $F_{\text{GRF}x}$ and $F_{\text{GRF}y}$ during the single stance phase was computed. The results are shown in Fig. A17. The relative size of $F_{\text{GRF}x}$ with respect to $F_{\text{GRF}y}$ increases significantly when the unloading increases. Fig. A18 shows that the mean value of $F_{\text{GRF}x}$ decreases significantly with unloading. The median values of $F_{\text{GRF}x}$ for the unloading conditions were 3.5% BW for 20G, 2.7% BW for 40G, and 1.7% BW for the 60G condition (see Appendix K Fig. A18).

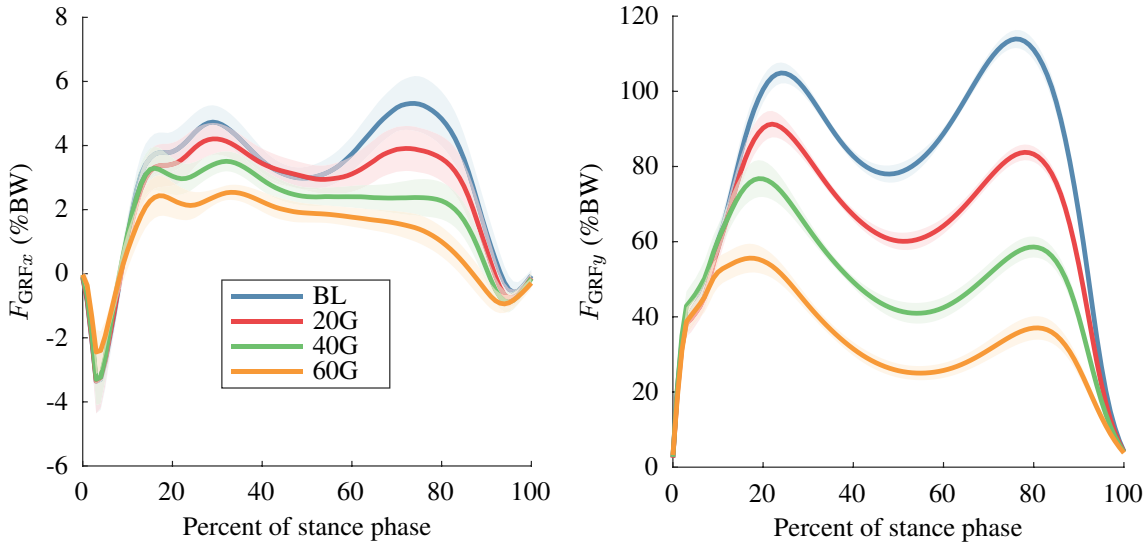

Fig. A16. The two figures show the mean trajectory of $F_{\text{GRF}x}$ and $F_{\text{GRF}y}$ during the stance phase. The shaded regions represent the 95% confidence interval of the mean trajectory.

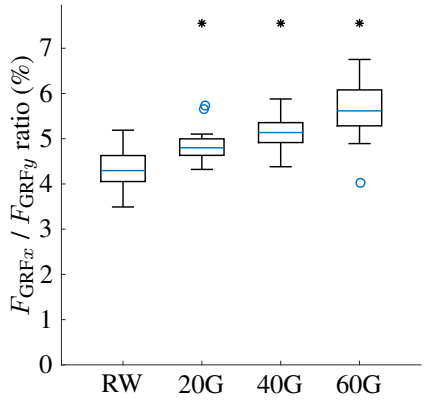

Fig. A17. Ratio between $F_{\text{GRF}x}$ and $F_{\text{GRF}y}$ during the single stance phase.

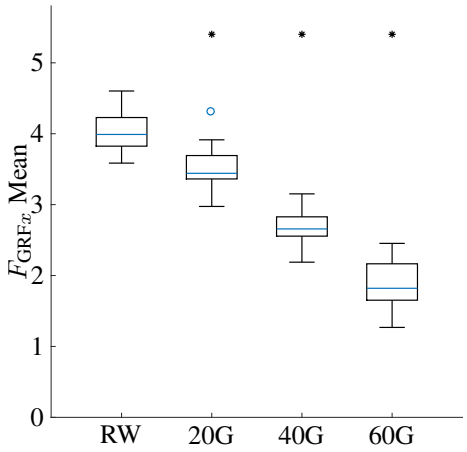

Fig. A18. The mean value of $F_{\mathrm{BWS}x}$ across the single-stance phase of walking. An asterisk (*) denotes a significant difference to the RW condition.

L: Secondary outcome measures

Step lengths were defined as the anterior-posterior distance between the heel markers during the middle of double support for both the. Walking speed was computed by dividing the distance travelled by the CoM during the FP Strideby the stride time. The cadence was computed by dividing the 2 steps taken during the FP Strideby the stride time. Double Support was quantified as a percentage of the total stride time.

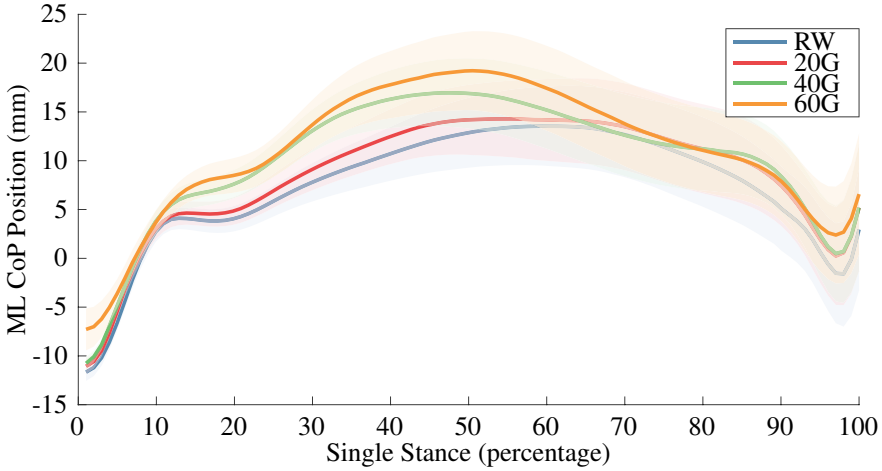

Fig. A19. Mean trajectory of the CoP below the foot during the single stance phase. The shaded regions represent the 95% confidence interval of the mean.

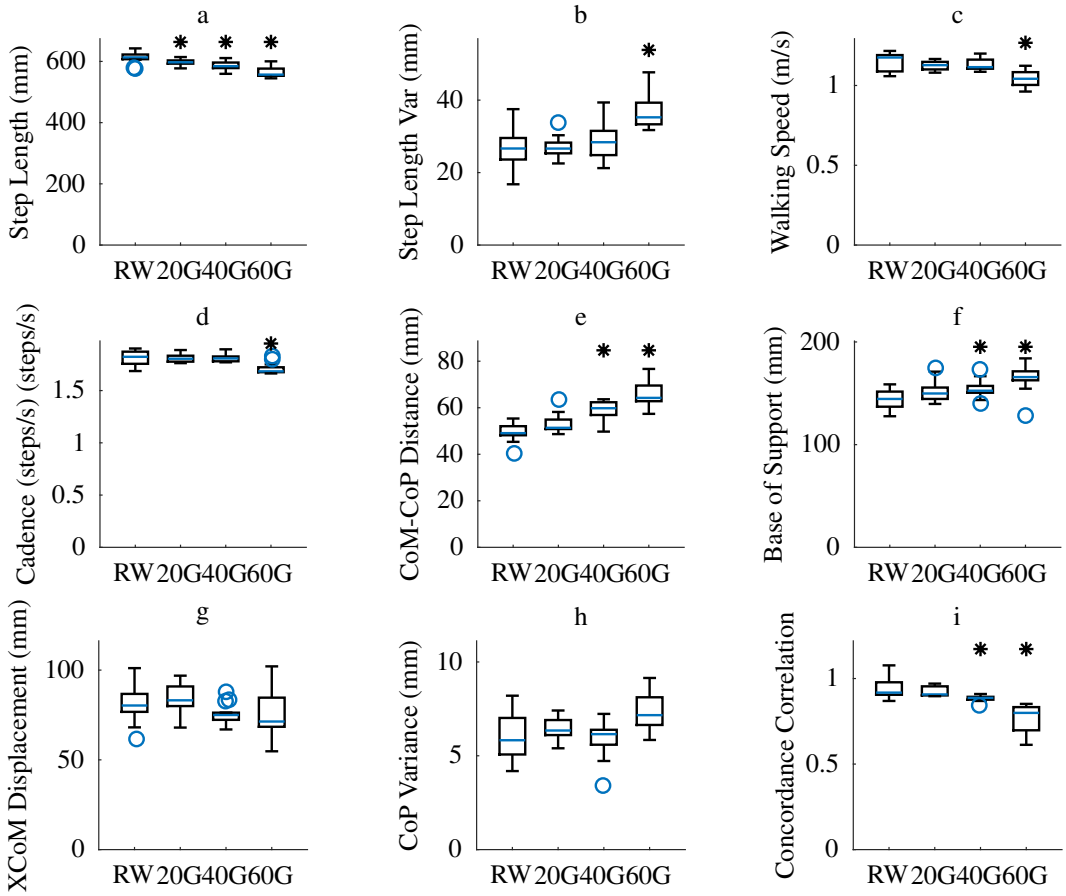

Fig. A20. Boxplots of the effect of vertical unloading on several secondary outcome measures. The between subject variance has been removed in these plots. An asterisk (*) above the boxplot indicates a significant difference to the RW condition.)

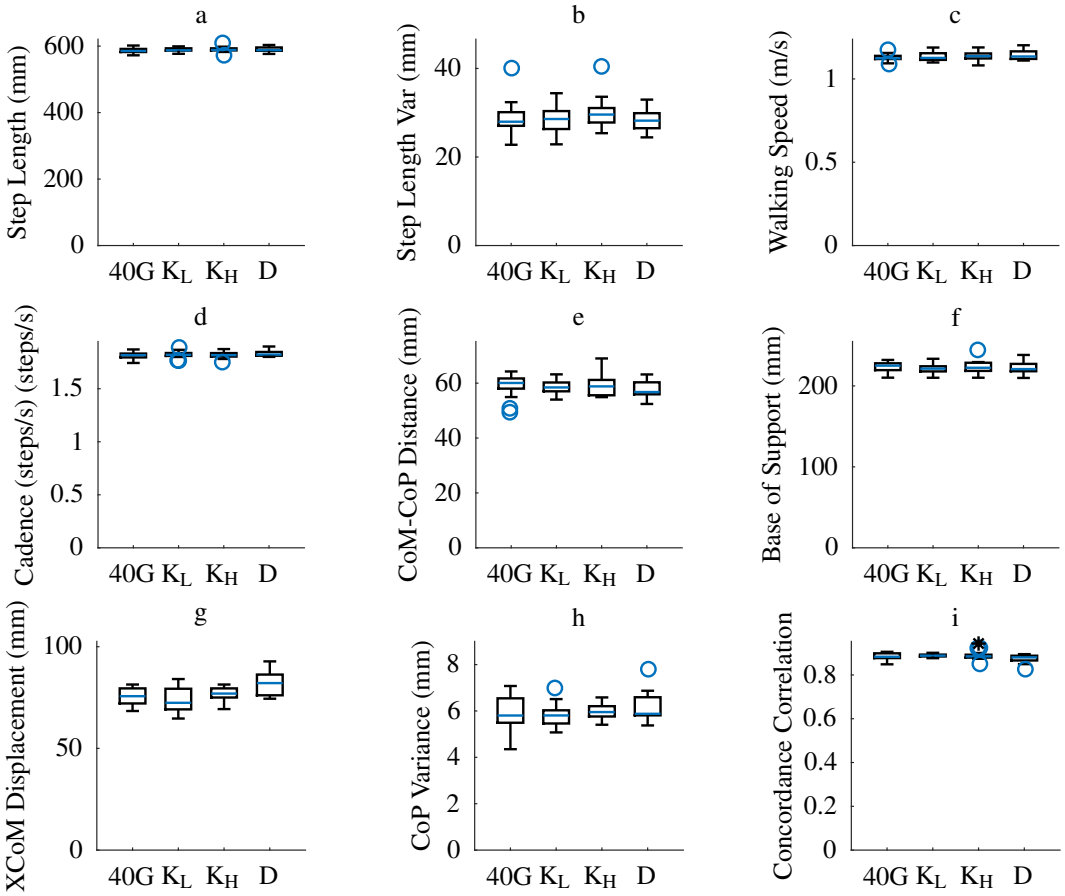

Fig. A21. Boxplots of the effect of lateral support on several secondary outcome measures. The between subject variance has been removed in these plots. An asterisk (*) above the boxplot indicates a significant difference to the RW condition.)

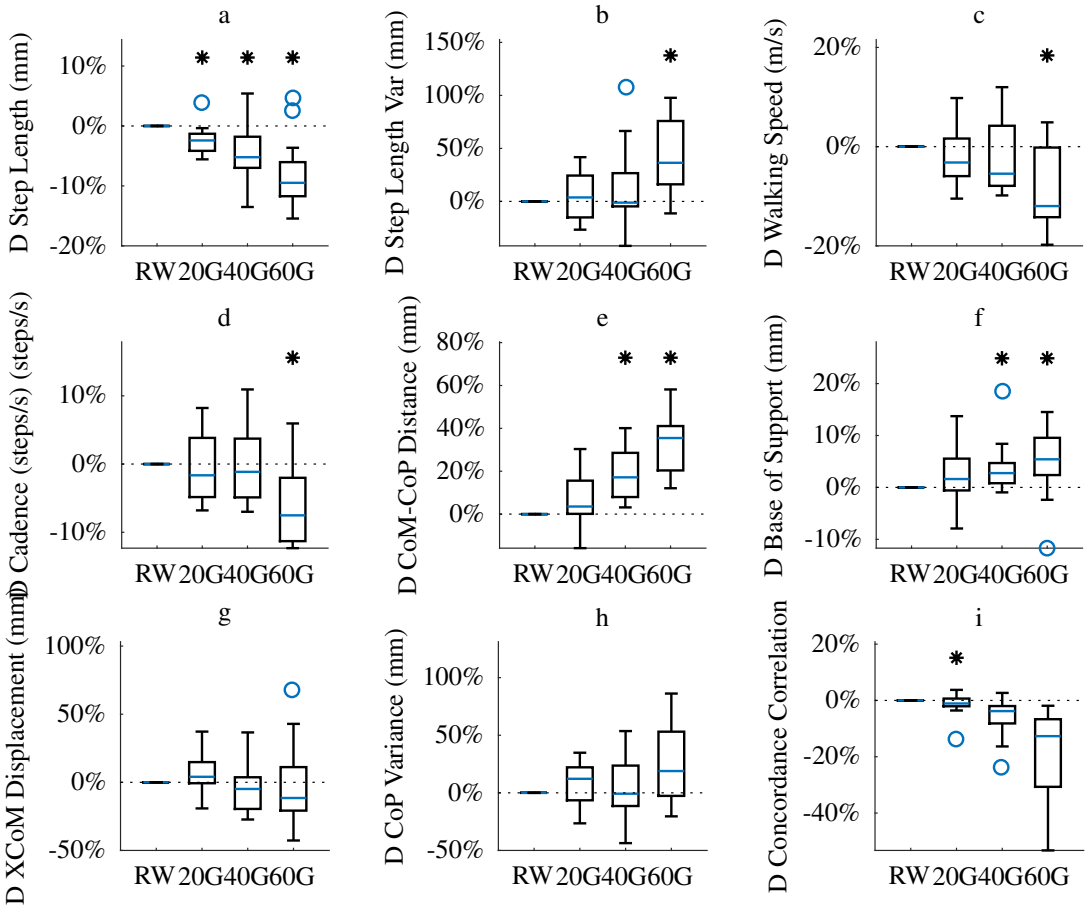

Fig. A22. Boxplots of the effect of vertical unloading on the outcome measures. The y-axis represents the relative difference to the RW condition. An asterisk (*) above the boxplot indicates a significant difference to the RW condition.

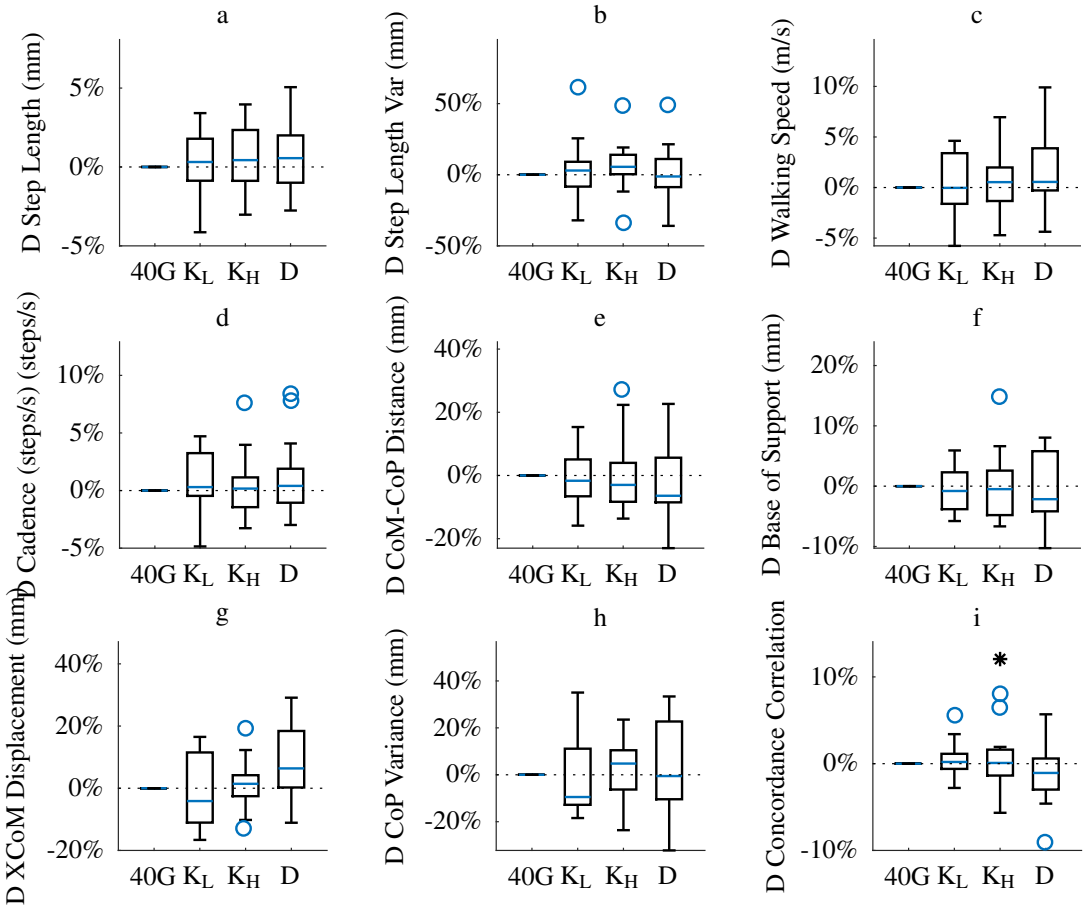

Fig. A23. Boxplots of the effect of vertical unloading on the outcome measures. The y-axis represents the relative difference to the 40G condition. An asterisk (*) above the boxplot indicates a significant difference to the RW condition.